



HAL
open science

Paravani, a puzzling lake in the South Caucasus

Erwan Messenger, Jérôme Poulénard, Pierre Sabatier, Anne-Lise Develle,
Bruno Wilhelm, Sébastien Nomade, Vincent Scao, Charline Giguet-Covex,
Ulrich Von Grafenstein, Fabien Arnaud, et al.

► **To cite this version:**

Erwan Messenger, Jérôme Poulénard, Pierre Sabatier, Anne-Lise Develle, Bruno Wilhelm, et al..
Paravani, a puzzling lake in the South Caucasus. *Quaternary International*, 2021, 579, pp.6-18.
10.1016/j.quaint.2020.04.005 . hal-03066916

HAL Id: hal-03066916

<https://hal.science/hal-03066916>

Submitted on 23 Nov 2021

HAL is a multi-disciplinary open access archive for the deposit and dissemination of scientific research documents, whether they are published or not. The documents may come from teaching and research institutions in France or abroad, or from public or private research centers.

L'archive ouverte pluridisciplinaire **HAL**, est destinée au dépôt et à la diffusion de documents scientifiques de niveau recherche, publiés ou non, émanant des établissements d'enseignement et de recherche français ou étrangers, des laboratoires publics ou privés.



Distributed under a Creative Commons Attribution - NonCommercial - NoDerivatives 4.0
International License

1 **Paravani, a puzzling Lake in the South Caucasus**

2

3 Erwan Messenger (a), Jérôme Poulénard (a), Pierre Sabatier (a), Anne-Lise Develle (a), Bruno Wilhelm
4 (b), Sébastien Nomade (c), Vincent Scao (c), Charline Giguët-Covex (a), Ulrich Von Grafenstein (c),
5 Fabien Arnaud (a), Emmanuel Malet (a), Ana Mgeladze (d), Estelle Herrscher (e), Mathilde Banjan (a)
6 Arnaud Mazuy (f), Jean-Pascal Dumoulin (g), Soumaya Belmecheri (h), David Lordkipanidze (d).

7

8 a. EDYTEM, Université Savoie Mont-Blanc, CNRS, Le Bourget du Lac

9 b. University Grenoble Alpes, LTHE, 38 000 Grenoble

10 c. LSCE/IPSL, Laboratoire CEA-CNRS-UVSQ et Université de Paris-Saclay Domaine du CNRS, Bât. 12,
11 Avenue de la Terrasse, 91198 Gif sur Yvette, France

12 d. Georgian National Museum. 3, Rustaveli Avenue, 0105 Tbilisi.

13 e. Aix Marseille Univ, CNRS, Minist Culture, LAMPEA, Aix-en-Provence, France

14 f. UMR 7264, CEPAM-CNRS Nice Université. Campus SJA3, 06357 Nice Cedex 4

15 g. UMS 2572, Laboratoire de Mesure du Carbone 14. CEA Saclay, 91191 Gif sur Yvette

16 h. Laboratory of Tree-Ring Research, 1215 East Lowell Street, Tucson, AZ 85721

17

18 **Abstract**

19 Sediments of Lake Paravani, the largest natural lake in the South Caucasus, were analysed to
20 reconstruct the millennial history of the environment. Pollen analysis, previously undertaken on the
21 first core retrieved in the middle of the lake, revealed a vegetation history for the last 12 millennia.
22 As part of the present study, a new core was taken from the north-western part of the lake. Pollen
23 analysis was performed on this new core with the same methodology as for the previous one. A
24 sedimentological and geochemical analysis was also conducted on both cores in order to gain an
25 understanding of the dynamics of erosion in the catchment area in response to landscape
26 modifications. The results show that the sediment deposits within Lake Paravani yield rather complex
27 and puzzle-like palaeoecological records. Despite the differences between the two records,
28 correlations have been made that are supported by the ^{14}C dates. By combining all of the data from
29 both cores, it was finally possible to reconstruct the puzzle of the environmental history recounted
30 by the Lake Paravani sediments. This reconstructed history is composed of four main phases: 1. a
31 steppic environment marked by pronounced erosion processes from 12 000 to 10 000 cal. BP; 2. a
32 transition phase characterized by the expansion of grasses (Poaceae) from 10 000 to 9-8 000 cal. BP;
33 3. a more forested phase from 9-8 000 to 2 000 cal. BP, during which the erosion fluxes decreased;
34 and 4. a decline in tree cover probably due to human activities over the last 2 millennia.

35

36 **Introduction**

37 The South Caucasus is located at the crossroads of Europe, the Middle East and Central Asia (Fig. S1)
38 and provides an original archaeological chronicle, influenced both by its proximity to the Levant (the
39 cradle of agriculture in Europe), and its specificity as a mountainous region. Therefore, the question
40 of the environmental trajectories in the South Caucasus is crucial for understanding the regional
41 demography and the socio-economic dynamics of past societies. Well-dated palaeoecological records
42 are scarce and the vegetation history is not yet fully-understood. A research effort has been
43 conducted in this region over the last ten years to reconstruct the history of palaeoenvironments,
44 and in particular the vegetation (Connor and Sagona, 2007; Ammann, 2009; de Klerk et al., 2009;
45 Connor, 2011; Messenger et al., 2013, 2017; Joannin et al., 2014; Leroyer et al., 2016; Connor et al.,
46 2018). Sites favourable to sediment archiving, such as lakes, are particularly targeted. Lake Paravani,
47 located on the Javakheti Plateau, is the largest lake in Georgia and was the subject of an early study
48 (Messenger et al., 2013). In this previous work, the vegetation history was reconstructed based on one
49 core sampled in the middle of the lake. This method, based on one core, is common practice in
50 palaeoecological studies using lake sediment (Cohen, 2006). Based on this study, a three-phase
51 vegetation history emerged for the Javakheti Plateau: 1. a steppic environment under a cold and arid
52 climate from 12 000 to 8 500 cal. BP, 2. a more forested environment from 9-8 000 to 2000 cal. BP
53 and 3. a decline in tree cover during the last 2 millennia due to human impact.

54 Other pollen analyses carried out in similar contexts (volcanic plateaux in the Lesser Caucasus,
55 elevation close to 2000m) also revealed a major palaeoecological change (transition from steppe to
56 more forested and/or increasing hygrophilous vegetation) which occurred at 9-8 000 cal. years BP
57 (Joannin et al., 2014; Leroyer et al., 2016; Messenger et al., 2017). In South-western Georgia, a region
58 close to the Black Sea, which represents a major source of moisture, the vegetation history seems to
59 differ somewhat, with forest expansion occurring earlier, around 10 000 cal. BP at an elevation of
60 2000 m asl (Margalidze, 1995; Connor et al., 2018).

61 Over recent years, we have collected several other cores from Lake Paravani with two objectives: 1.
62 to better understand the sediment processes in this large, shallow lake and 2. to find sediments
63 dating to the Early Holocene that might help us to clarify the question of forest expansion in that
64 region (chronology, climatic control, etc.). Most of the retrieved sequences are fragmentary (with
65 many hiatuses) or are very short (Fig. S2). In this paper, we propose to analyse and compare the two
66 longest and most complete sequences from Paravani. A multiproxy approach combining
67 sedimentology and mineral geochemistry was adopted to gain a better understanding of the
68 relationships between the lake sediment records and the erosive processes that have affected the
69 watershed. New pollen analysis was undertaken on core PAR12-04 and the results were compared to

70 pollen data from the previously published core PAR09-01. Finally, based on the sediment and pollen
71 data, we have been able to reconstruct the chronology and the patterns of the Paravani deposits.
72 The overall goal of this study is to improve scientific knowledge of the climate and vegetation
73 histories of the highlands, and to understand their relationships with the erosive processes and the
74 functioning of the lake over the last 12 millennia.

75

76 **Regional and local setting**

77 Lake Paravani is located on the Samtskhe-Javakheti Plateau, at 2073m a.s.l., between two main
78 volcanic domains (Fig. 1). The eastern part is dominated by old (3-1 Ma) basaltic lavas and andesitic
79 basalts (Nomade et al., 2016), composed of less differentiated and under-saturated Ti rich rocks
80 (Javakheti plateau, *sensu stricto*). The western part is mainly composed of differentiated rocks such as
81 dacites and andesites. These rocks all belong to the most recent activity (last 500 ka) of the Samsari
82 Ridge (Lebedev et al., 2008, Nomade et al., 2016). This volcanic ridge (Fig. 1) corresponds to 20
83 principal volcanic domes. The watershed (234 km²) of Lake Paravani (surface of 37.5 km²) straddles
84 the two main volcanic units.

85

86 The Javakheti region possesses the largest number of lakes and marshes within the Caucasus
87 (Matcharashvili et al., 2004). Inherited glacial morphologies and formations are widespread on the
88 Javakheti Plateau, but no active glacier currently exists. The climate of the Javakheti Plateau is
89 continental with long, cold winters and short, cool summers. The mean annual temperature is ca.
90 5.3°C and the annual precipitation rate is ca. 500-600 mm with a maximum in late spring and early
91 summer, and a minimum in January (Matcharashvili et al., 2004). The most widely distributed
92 vegetation community is mountain steppe, dominated by grasses (Poaceae family, e.g. *Festuca* spp.
93 or *Stipa* spp., Fig. 2). Forest communities are mostly absent from the plateau and only two small
94 areas of sub-alpine forest still exist, one on the eastern part of Lake Kartsakhi and a second on the
95 side of Mt Tavkvetili (Fig. 2) (Arabuli et al., 2008). While the plateau is steppic, different types of
96 forest exist nowadays on the northern ranges (Bohn et al., 2000).

97

98

99 **Material and methods**

100 **1. Coring sites**

101 In this study, we investigate two cores collected in lake Paravani (Fig. 1): core PAR09-01 retrieved in
102 2009 from the middle of the lake at a water depth of 3 m (Messenger et al., 2013) and a new core
103 PAR12-04 retrieved from the littoral area at a water depth of 2.8 m (41.465°N, 43.799°E) in 2012.

104

105 **2. XRF core scanner**

106 The relative major element contents were measured every 0.5 cm on PAR09-01 and PAR12-04 using
107 a XRF Avaatech core scanner (EDYTEM laboratory, Université de Savoie Mont-Blanc). An X-Ray beam
108 was generated with a rhodium anode and a 125 µm beryllium window which allows a voltage range
109 of 7 to 50 kV and a current range 0 to 2 mA. The analytical settings were adjusted at 10 kV and 1.5mA
110 in order to detect light elements (Al -> Fe). Each individual power spectrum was transformed by the
111 deconvolution process into relative contents (intensities) expressed in counts per seconds (cps).
112 Principal component analysis was applied to XRF data in order to decipher sedimentary processes
113 controlling the lake sedimentation using R statistical software and the multivariate analysis package
114 FactomineR (Fox, 2016; Lê et al., 2008; R Core Team, 2018).

115

116 **3. Magnetic Susceptibility**

117 For magnetic susceptibility (MS) analyses, two different protocols were used. The core 09-01 was
118 sampled using 2cm³ sampling plastic cubes at 2 cm resolution. The core PAR12-04 was sampled using
119 a U-channel. The U-channel was then directly measured with a 1 cm resolution. MS was measured at
120 the Laboratoire des Sciences du Climat et de l'Environnement (LSCE) at Gif-sur-Yvette (France) using
121 a Bartington® MS3 model, and the MS values obtained were normalized to sample weights (wet).

122

123 **4. Loss On Ignition analysis**

124 Loss On Ignition (LOI) analyses were carried out to estimate the organic content of the sediment,
125 following the procedure used by Heiri et al. (2001). Forty samples, collected at 1 to 3 cm intervals,
126 were dried. Since organic matter is oxidized to carbon oxide, dioxide and ash at temperatures
127 between ca. 200 and 500°C, the record of sample weights before and after heating (ignition at 550°C
128 during 5h) allows us to estimate the weight of the organic content. The heating of several test
129 samples to 950°C (for a period of 2h) in order to estimate the carbonate content yielded so negligible
130 a weight loss (<1%) that this step of the process was abandoned.

131

132 **5. Chronology**

133 The core chronology for PAR09-01 and PAR12-04 is based on 10 and 16 AMS ¹⁴C dates respectively,
134 determined on bulk sediment (Table 1).

135

136 Clam v2 (Blaauw, 2010), written for the open-source statistical software 'R', was used to calibrate the
137 ¹⁴C ages with the Intcal13 calibration curve (Reimer et al., 2013) and to construct an age-depth model
138 for cores PAR09-01 and PAR12-04. An age-depth model, already published for core PAR09-01 core

139 (Messenger et al., 2013), has been refined using Clam v2 software, based on the IntCal13 calibration
140 curve (Reimer et al., 2013).

141

142 **6. Pollen analysis**

143 Thirty-three samples were taken at 1 to 5 cm intervals for pollen analyses. For each sample, 1-2 g of
144 sediment were processed following standard methods in palynology, using HCl, KOH baths (Faegri
145 and Iversen, 1989) and heavy liquid (d:2) flotation (Girard and Renault-Miskovsky, 1969; Goeury and
146 Beaulieu, 1979). If significant amounts of silica particles remained, a HF bath was used. After
147 treatment, the residue was suspended in glycerol, mounted onto microscope slides and counted
148 using "Zeiss standard™" and "Leica DM 1000" microscopes. Pollen grains were identified using
149 atlases of European and Mediterranean pollen types (Reille, 1992; Beug, 2004). The pollen
150 concentration ranges from 10 to 30,000 grains. g⁻¹ in the A12 unit, from 30 to 60, 000 for the B12
151 unit, and from 60 to 250, 000 for the C12, D12 and E12 units. The total pollen sum ranges from 300
152 to 349 in most samples, except five samples in which pollen grains were less abundant: i.e. samples
153 72, 86, 92, 96, and 99 (from 205 to 270 pollen grains counted). Percentage calculations were based
154 on the total terrestrial pollen (AP: Arboreal Pollen + NAP/Non Arboreal Pollen), excluding
155 Cyperaceae, and moss and Pteridophyte spores.

156

157

158 **Results and Interpretation**

159 **1. Sediment analysis**

160 *Lithology and sediment description*

161 The stratigraphy of PAR12-04 is divided into five different units (A12 to E12) from the base to the top
162 of the sequence (Table 2, Fig. 3). Initially the unit boundaries were visually identified, and then they
163 were compared to the tipping point identified within the xrf data.

164

165 Sediment samples were collected in each unit to prepare smear slides. An illustrative picture of bulk
166 sediment for each unit is presented along the stratigraphy in the supplementary Fig. 3. The
167 observations of the slides provide an estimation of diatom abundance in each unit. All units contain a
168 significant quantity of diatoms, except unit A12, which is diatom-free. The richest units are B12 and
169 D12. The lithology of core PAR09-01 (Fig. 3) has already been described by Messenger et al. (2013).
170 The three initial units A, B, C have been renamed A9, B9 and C9 for this paper (Table 2). Following the
171 same methodology used for PAR 12 04, the boundary between units B9 and C9 has been moved by
172 2.5 cm (29 cm instead of 31.5 cm) based on the shift recorded at 29 cm by XRF data.

173

174 *LOI analysis*

175 The LOI tests at 950°C did not reveal significant carbonate content in the Paravani sediment. The LOI
176 at 550°C is presented in figure 3. For core PAR 12-04, the LOI is lower than 10% for the lowest units
177 A12 and B12. The LOI values fluctuate from 12 to 16% for C12, from 10 to 12% for D12 and from 10
178 to 18% for E12. For core PAR 09-01, units A9 and B9 present low contents of organic matter. The
179 highest LOI values (up to 12%) are recorded in the upper unit, C9.

180

181 *Magnetic susceptibility*

182 For core PAR12-04, the magnetic susceptibility displays high values for units A12 and B12, lower
183 values for C12 and D12, and a progressive increase within unit E12 (Fig. 3). The magnetic
184 susceptibility curve for PAR09-01 has already been described elsewhere (Messenger et al., 2013).

185

186 *XRF analysis*

187 *Down core variations*

188 Al, Si, K, Ca, Ti and Fe XRF intensities are presented in figure 3 for both cores. In PAR09-01, all
189 elements reach their highest values in A9 (Fig. 3). In B9 and C9, they decrease gradually up to the top
190 of the sequence. In PAR12-04, the highest values for all XRF indicators are observed in A12 and B12.
191 Detrital inputs then decrease gradually from C12 up until the upper 10 cm of E12, where they

192 decrease again sharply. Surprisingly, this decrease occurs for all elements and seems to be due to a
193 water content effect. All elements roughly follow the same trend in both cores, except for small
194 variations that are particularly perceptible in the calcium XRF signal.

195 *Principal component analysis*

196 Principal component analysis (PCA) was applied to the XRF results in order to decipher sedimentary
197 processes controlling the geochemistry of cores PAR09-01 and PAR12-04 (Fig. 4). PCA was performed
198 on major elements (Al, Si, K, Ti, Ca and Fe intensities). In both cores, nearly 80% of the total variance
199 is supported by high loadings of all elements on dimension 1 (Dim1). This could be due to a strong
200 imprint of detrital inputs and the absence of other XRF indicators, which could be associated with
201 other processes (organic production and/or redox variations). However, variable projections for both
202 cores indicate a similar trend between two end-members in the detrital inputs, which could be
203 associated with a balance of fine to coarse particles (e.g. Fe and K against Ca and Si), and/or
204 geochemical changes due to changes in source of sediments (Sabatier et al., 2010; Wilhelm et al.,
205 2016a).

206

207 Individual projections are sorted by units (Fig. 4). In PAR09-01, unit A9 is strongly supported by Dim1,
208 which indicates that detrital processes dominate the signal in this unit (mainly K, Al, Fe
209 contributions). Conversely, in unit B9 and then in C9, we observe a gradual shift toward a negative
210 correlation to Dim1; this indicates that these units are characterised by less detrital inputs and other
211 controlling processes. In PAR12-04, the trajectory scheme of the unit is roughly the same as for
212 PAR09-01, with a strong correlation of A12 individuals to Dim1 and then a gradual shift to negative
213 loadings from B12 to E12.

214 *Geochemical relationships\ratios*

215 Based on the XRF data, three ratios have been calculated: Si/Al (Fig. S3), Fe/Al and Ti/Al (Fig. S4).

216 - The Si/Al ratio can be considered as a tracer of biogenic silica (Köning et al., 2002, Ragueneau et al.,
217 2005). In PAR09-01, the Si/Al ratio is low in A9, and increases sharply at the transition between A9
218 and B9. It remains stable in B9 and C9, except in the 40-20 cm interval where higher values are
219 observed. In PAR12-04, the Si/Al ratio is low in A12 and increases slightly in B12. It exhibits
220 fluctuations between high values in B12 and D12 and lower values in A12, C12 and E12. Finally, a
221 gradual increase is observed in the upper 10cm interval of the core.

222 In the Paravani sequence, the Si/Al ratio covariates with diatom abundance (Fig. S3) and closely
223 matches the other indicators of climate improvement (pollen, OM, etc.). We could interpret it as a

224 first marker of biogenic silica, but it should be used with caution because the Si contribution of the
225 bedrock can also modify the Si/Al.

226 - The Ti/Al and Fe/Al ratios have been tested in order to decipher the different sources of the mineral
227 input (See Fig. S4). Different volcanic formations, such as basalt-basaltic andesite and dacite-
228 andesite, occur in the Paravani watershed (Fig. 1). Because the basalt-basaltic andesite is rich in Ti
229 and Fe (Nomade et al., 2016), the rise in Ti/Al and Fe/Al ratios could be interpreted as indicating a
230 greater contribution from these formations in the detrital input. Both ratios exhibit the same trend
231 (Fig. S4). In PAR09-01, the values are low in A9, increase slightly in B9 and increase simultaneously in
232 C9. In PAR12-04, Fe/Al and Ti/Al ratios are relatively stable and remain low all along the sequence,
233 except towards the top of the sequence, where they both increase sharply. They yield an ambiguous
234 signal that is probably influenced by the double origin of the silica (bedrock and biogenic silica). Thus,
235 the core scanner XRF data do not permit us to carry out source analysis satisfactorily. It is for this
236 reason that the specific task of quantifying detrital and biogenic inputs will be undertaken using WD-
237 XRF.

238 Overall, in the case of this study of the Paravani sediments, the XRF core scanner is used to some
239 extent as a correlation tool and as a preliminary indicator of biogenic silica contribution.

240

241 *Chronology*

242 Sixteen radiocarbon measurements were performed on organic matter from bulk sediment collected
243 in core PAR12-04 (Table 1). Among the 16 samples analysed, one date was rejected from the age-
244 depth model (Fig. 5); the Poz58699 sample at 93.5 cm (Table 1), dated to 11240 BP, is clearly too old,
245 probably due to the presence of reworked material.

246 A number of hiatuses have been identified based on the combination of radiocarbon ages and abrupt
247 changes in geochemistry (XRF data). Two main hiatuses were identified at depths of 84.5 cm
248 (between B12 and C12) and 69 cm (between C12 and D12). Deposition of the C12 unit began around
249 5 100 and stopped at 4 650 cal. year BP. A hiatus of 1 850 years precedes the onset of the deposition
250 of D12 at around 2800 cal. years BP. The other hiatus, which occurs between units B12 and C12, lasts
251 more than 4 000 years.

252

253 For core PAR09-01, ten samples were radiocarbon dated (Messenger et al., 2013). Based on pollen and
254 XRF data, the B12 phase recorded in PAR12-04, ranging from 10 500 to 9 300 cal. years BP, is not
255 recorded in the PAR09-01. As a result, a hiatus has been proposed at a depth of 69 cm (Fig. 5). The
256 underlying sediments are older (two radiocarbon dates earlier than 12 000 cal. years BP) and the
257 continuous record begins at 69cm, or at 8250 cal. years BP (Fig. 5).

258

259 **2. Pollen results**

260 Results of the pollen analyses are presented in the pollen diagram below (Fig. 6). Local Pollen
261 Assemblage Zones (LPAZ) have been defined (Birks and Birks, 1980) using the CONISS method
262 (Grimm, 1987). Five main LPAZs have been identified in the PAR12-04 pollen record (Fig. 6):

263

264 - LPAZ1 (depth: 105.5-91 cm): The first zone is characterized by the prevalence of herbaceous pollen
265 taxa. Amaranthaceae-Chenopodiaceae (42.9-56.8%) and *Artemisia* (12.7-24.3%) dominate the pollen
266 assemblages. Open vegetation is also attested by the abundance of other herb taxa, such as Poaceae,
267 Asteraceae (Asteroideae, Cichorioideae), Caryophyllaceae. The Alimsataceae family is well
268 represented (1.5-7%). The xeric and steppic taxon, *Ephedra distachya* t., is present in every sample of
269 this zone (0.5-2.4%). In this LPAZ, just a few tree pollen grains of *Betula* (0.4-1%), *Quercus* (0.5-1.5%),
270 *Fagus* (0-0.8%), *Pinus* (0-1.5%) and *Corylus* (0-0.5%) have been identified.

271 - LPAZ2 (depth 91-85 cm): This zone is marked by an abrupt decrease of Amaranthaceae-
272 Chenopodiaceae (17.6-26.2%), while Poaceae values rise significantly, from 18.5% to over 33%. There
273 is a slighter decrease in *Artemisia* while the other herbs present rather stable pollen values. This zone
274 records the last significant occurrence of the Alimsataceae family. The AP values increase (from 14.7
275 to 28.9%) in LPAZ 2 due to the progressive expansion of deciduous trees such as *Quercus*, *Fagus*,
276 *Betula* and *Carpinus*. Nonetheless, *Ephedra distachya* is still well represented, attesting to the steppic
277 character of the vegetation.

278 - LPAZ3 (depth 85-68 cm): This zone is characterized by low values of herbaceous pollen (NAP ranges
279 from 35.8 to 50.6%) and high pollen values for tree pollen taxa, such as *Pinus* (19.3-35.2%), *Betula*
280 (1.9-3.4%), *Carpinus* (2.3-7.1%), *Fagus* (3.8-6.9%), and *Quercus* (10-15%). *Ephedra distachya* is not
281 recorded.

282 - LPAZ4 (depth 68-58cm): This zone is marked by the lowest herbaceous pollen values of the record
283 (NAP ranges from 21 to 26.6%) due to low Poaceae, Amaranthaceae-Chenopodiaceae and *Artemisia*
284 pollen values. LPAZ4 is also characterised by the highest values of *Pinus* in the sequence (36.8-52%).

285 - LPAZ5 (depth 58-0cm): In this zone, some of the herbaceous pollen taxa, such as Asteraceae
286 Asteroideae, Ast. Cichorioideae and Poaceae, show increasing frequencies. Pollen indicators of
287 human activities display a continuous curve (Fig. 9). Indeed, the taxa *Plantago*, an indicator of
288 pastoral activity, and *Cerealia* are both well recorded in this zone. Deciduous trees present stable
289 pollen values, but the *Pinus* values tend to decrease slightly along the LPAZ. *Abies* tends to disappear
290 while *Picea* presents increasing pollen values. This zone documents a more open landscape than
291 LPAZ4.

292

293 Discussion

294 1. Why a puzzling lake?

295 The sediment analysis of PAR12-04 and PAR09-01 sequences shows that the deposits within Lake
296 Paravani yield rather complicated and puzzle-like palaeoecological records. To reconstruct the history
297 of past environments, palaeoecologists traditionally use the sediments recovered from the deepest
298 and/or central part of the lake (Cohen, 2003). Such a sequence is assumed to be representative of
299 the lake deposits. Since the sequence comes from the lowest bathymetric point (lowest bottom), the
300 occurrence of hiatuses due to very low sedimentation, or none at all, during emerging phases is
301 limited. Even though, core PAR09-01 was taken from the central part of the lake, and at the
302 maximum depth (3m), its sequence presents a hiatus of several thousands of years at a depth of 69
303 cm (Fig. 5). Indeed, when comparing the pollen data from both cores, the period covered by the B12
304 unit in PAR12-04 (10 500 to 9 300 cal. years BP), characterized by very high Poaceae values and a
305 slight increase of arboreal taxa, is not recorded in PAR09-01 (Fig. S5). The absence of a hiatus for this
306 time period in core PAR12-04, a core retrieved in a slightly higher bathymetric point (2.8m), is an
307 unexpected result because in theory, this upper point, located closer to the shoreline, is more likely
308 to be affected by emerging phases. The PAR12-04 sequence presents hiatuses of 4 000 and 1 850
309 years at depths of 84.5 and 69 cm, respectively. Consequently, both cores yield two different records
310 with asynchronous hiatuses. Correlating the different units turned out to be a real challenge. The
311 curves provided by XRF core logging (which is an efficient tool for correlating lake sequences) were
312 not easy to disentangle (Fig. 3). Their comparison is rendered particularly complex by the hiatuses
313 and variable concentrations of diatoms (Fig. S3). Indeed, the increasing diatom concentration dilutes
314 the detrital input and may have a significant effect on the XRF results (dilution of other elements by
315 biogenic silica). If the diatom bloom is localized in the lake, some cores might record diatoms while
316 others would not. Dissimilar sediment sequences within a single lake have already been observed in
317 several lakes (Anderson, 1986; Beaudoin and Reasoner, 1992). However, in previous works, the cores
318 came from different depths (contrasted bathymetry). In the case of Lake Paravani, the lake bottom is
319 almost flat and there is no delta which might generate significant differences in sediment facies. The
320 presence of hiatuses at Paravani could be explained by the low water depth (facilitating bottom
321 emergence during low lake levels), but how do we explain the absence of synchronicity for these
322 hiatuses? One hypothesis that might be forwarded is the effect of earthquakes. In fact, lacustrine
323 sedimentation can be highly sensitive to regional earthquake activity with slope failures, violent
324 waves and seiche effects causing hiatuses (Chapron et al., 2016, Wilhelm et al., 2016). In the
325 Samskhe-Javakheti, which is known as a seismically active region (Kachakhidze et al., 2003), past
326 earthquakes could have modified the lake sedimentation. Numerous prehistoric and historical
327 earthquakes have already been documented in the region (Philip et al., 2001; Ritz et al., 2016). No

328 traces of homogenite or turbidite have been observed in the sequences. Moreover, in such a large
329 and shallow water body, it is difficult to imagine that the observed hiatuses could be the result of
330 mass wasting deposits (displaced blocks of sediment), an earthquake-triggered mechanism that has
331 been clearly identified in the Alps (Wilhelm et al., 2016). The Paravani Lake seems to be on a major
332 fault (Nomade et al., 2016), within a highly seismically active area, where earthquakes of a 6-7
333 magnitude and surface ruptures are historically attested (Ritz et al., 2016). Without detailed
334 bathymetry mapping, however, we cannot discuss the potential of underwater fault activity leading
335 to sediment hiatuses in the upper compartments (Beck et al., 2012). Another factor that could have
336 played a role in the sedimentation process is the wind. In shallow lakes, such as Paravani, the wind
337 can directly drive the sedimentation process and hydrodynamics, generating deep erosional surfaces
338 (Nutz et al., 2016). This question deserves further exploration because Paravani is particularly subject
339 to thermal winds during the summer.

340 Despite the differences between the two records, it is possible to draw correlations (Fig. 7 and 8)
341 based on pollen data and the PCA performed on the XRF data (Fig. 4). These correlations are
342 supported by the ¹⁴C dates, thus allowing us to better constrain the chronology of each unit. By
343 combining all of the data from both cores, it is finally possible to reconstruct the puzzle of the
344 environmental history recounted by the lake Paravani sediments (Fig. 7).

345

346 **2. The environmental history provided by the combination of 09-01 and 12-04 records**

347 *Before 10 500 years cal. BP*

348 The A12 and A9 units are mainly composed of detrital sediment (Fig. S3), characterized by high Si, Ca,
349 Ti and Fe inputs (Fig. 3) that reflect erosion processes in the Paravani watershed. The low OM value
350 probably indicates low biogenic production in the lake. Diatoms are almost absent in this deposit
351 (low Si/Al and Fig. S3). At that time, the reconstructed vegetation is composed of steppes and semi-
352 desert steppes. All proxies indicate cold, arid climatic conditions. Regional records dating back
353 further than 10-11 000 years cal. BP are characterised by similar environmental and climatic
354 conditions (Wick et al., 2003; Litt et al., 2009; Van Zeist and Bottema, 1977). Such vegetation,
355 dominated by Amaranthaceae-Chenopodiaceae, is characteristic of glacial phases recorded in the
356 two long regional sequences sampled in Lakes Urmia (Djamali et al., 2008) and Van (Wick et al., 2003;
357 Litt et al., 2014). In the volcanic region of the Armenian-Javakheti plateau (Fig. S1), very limited tree
358 cover has been clearly demonstrated by both the Zarishat (Joannin et al., 2014) and Nariani pollen
359 records (Messenger et al., 2017).

360

361 *From 10 500 to 9 300 cal. years BP*

362 The phase recorded by unit B12 is probably the most interesting part of the PAR12-04 sequence. The
363 deposit is securely dated by three radiocarbon dates and fits well within the Early Holocene period,
364 10 500 to 9 300 cal. years BP (Fig. 7). This record was not recovered by the first sequence (PAR09-01)
365 sampled in Lake Paravani. The sediment of unit B12 is still characterized by detrital input due to
366 erosion. The sediment displays a very low content of organic matter. Nevertheless, the Si/Al curve
367 indicates an increase in biogenic silica, which is confirmed by the abundance of diatoms in smear
368 slides (Fig. S3). This means that the lake system was experiencing a change, with increasing bio-
369 production. Yet, at the same time, the quantity of organic matter remains low, meaning that not all
370 compartments of the lake system are responding at the same time. This change in lake production
371 may have various causes (e.g. rise in temperature, rise in lake level, etc.).

372 The pollen assemblages from this phase are marked by a very slight increase of tree pollen values
373 due to a small rise in deciduous trees (Fig. 8). This slight rise in taxa living at lower elevations
374 (*Quercus*, *Carpinus*, *Corylus*, etc.) reflects an initial and slight tree expansion in lower vegetation
375 belts, perhaps even from the western part of the South Caucasus (by long-distance pollen transport).
376 This record fits well with the synchronic expansion of deciduous trees recorded at 10 000 cal. BP (See
377 Fig. S6) in the Didachara sequence in south-western Georgia (Connor et al., 2017). Apart from this
378 regional pollen echo from western areas, the pollen assemblages from this phase are still dominated
379 by herbs (71-85-%). In Western Europe, the post-glacial expansion of temperate trees (Huntley and
380 Birks, 1983; Wick, 2000) was underway by this time, but in the South Caucasus, several records
381 indicate that the environment remained steppic in the early Holocene (Margalitzadze, 1995; Messager
382 et al., 2013; 2017; Joannin et al., 2014; Leroyer et al., 2016). This pattern is also observed in other
383 regions of South-Eastern Europe and the Near East (Van Zeist and Bottema, 1977, Bottema, 1986;
384 Stefanova and Ammann, 2003; Wright et al., 2003; Djamali et al., 2008; Djamali et al., 2010; Connor
385 et al. 2013; Leroy et al., 2013, 2014; Ryabogina et al., 2019). Different hypotheses have been
386 proposed to explain the delay in forest expansion: (1) the time lag in tree migration from glacial tree
387 refugia (Leroy et Arpe, 2007); (2) the impact of burning (Roberts, 2002; Turner et al., 2010); (3) a
388 relatively dry early Holocene climate (Stefanova and Ammann, 2003; Atanassova, 2005;
389 Shumilovskikh et al., 2012; Van Zeist and Bottema, 1991; Roberts and Wright, 1993; Stevens et al.,
390 2001, 2006; Wright et al., 2003; Djamali et al., 2010); and (4) a negative feedback from the “Black
391 Lake”, preceding the filling of the Black Sea by Mediterranean waters (Leroy et al., 2013). All of these
392 hypotheses have been addressed and discussed in the context of the neighbouring Nariani pollen
393 record (Javakheti Plateau) (Messager et al., 2017).

394 For this time period, pollen assemblages from the Paravani B12 unit indicate a major change in the
395 herb communities with a significant decrease of Amaranthaceae-Chenopodiaceae (Fig. 7), which was
396 the dominant taxon recorded at Paravani since 12 500 years cal. BP. This decline of Amaranthaceae-

397 Chenopodiaceae corresponds to the expansion of Poaceae (Fig. 7). A similar vegetation dynamic was
398 observed at Nariani between 10 200 and 9000 cal. years BP (Messenger et al., 2017). Such a pattern
399 (i.e. decline of semi-desert, expansion of grassland and very slight rise in tree cover) is also described
400 from the Lake Van sequence (Fig. S6) between 11 500 and 9000 cal. years BP (Wick et al., 2003; Litt
401 et al., 2009). This new pollen data from Paravani, dating back to the early Holocene, confirms the
402 vegetation history reconstructed in Nariani (Fig. 2, Fig. S6). Based on this change in the herb
403 community, a first climatic hypothesis was proposed (Messenger et al., 2017), namely that this period
404 is characterized by an increase in annual precipitation. Geochemical and isotopic indicators from
405 Lake Van (Lemcke and Sturm, 1997; Wick et al., 2003), Lake Eski Acigöl (Roberts et al., 2001; Jones et
406 al., 2007) and Nar Gölü (Dean et al., 2015) in Turkey (Fig. S1) show higher water levels and/or lower
407 salinities during the early Holocene. Based on these different indicators, significant annual rainfalls
408 were inferred for the early Holocene. While this climatic trend is regionally recognized, the first
409 Holocene coastal lake terraces on the shores of Lake Van have been dated to 9.5-6 ka (Kuzucuoğlu et
410 al., 2010; Çağatay et al., 2014), slightly younger than the other records. In Armenia, the first sign of
411 increasing rainfall is recorded a bit later (Joannin et al., 2014, Leroyer et al., 2016), around 8000 cal.
412 BP (Fig. S6). At a regional scale, the question of the early Holocene climate and its seasonality is still
413 unresolved. According to the Nariani and new Paravani pollen data, the growing season appears to
414 have remained dry (low precipitation during the spring, limiting tree expansion), while annual rainfall
415 increased. The change in the lake system recorded at Paravani (rising concentrations of diatoms)
416 could be interpreted as a sign of a higher lake level reflecting higher annual precipitation, but the
417 vegetation composition indicates that spring rainfalls remained low.

418

419 *From 8355 to 1600 cal. years BP*

420 This phase is only fully recorded by unit B9 in PAR09-01, while it is partly represented by units C12
421 and D12 in PAR12-04 (Fig. 8). The long phase recorded by the B9 unit is clearly marked by a drastic
422 change in sediment composition. As indicated by lower Ti and Fe values in XRF curves, the detrital
423 input decreased during this phase. The decline of erosion might be explained by the development of
424 soils in the watershed and the increasing vegetation cover (see below). The very high Si/Al values
425 could reflect higher biogenic silica production. During this period, both organic matter and biogenic
426 silica reveal higher lake production related to the climatic amelioration, which is, in turn, attested to
427 by the pollen record. Indeed, pollen assemblages reflect relatively forested vegetation growing under
428 warmer and wetter climate conditions. The period ranging from 8000 to 5500 cal. BP is recognized as
429 the period of maximum tree extension in the South Caucasus (Kvavadze and Connor, 2005; Connor
430 and Kvavadze, 2008). In the Paravani record, the pollen data does not reveal a significant human
431 impact from 8355 to 3000-2500 cal. BP (Fig. 8). This observation is rather unexpected because

432 numerous archaeological sites dating from the Neolithic to the Bronze Age have been identified on
433 the Javakheti Plateau in recent decades. While the Neolithic and Chalcolithic sites mainly occurred in
434 lowlands (Lyonnet et al., 2016; Hamon et al., 2016; Kadowaki et al., 2015), some sites have been
435 discovered on the volcanic plateaus. A rockshelter called Bavra-Ablari, located in the Paravanistkali
436 Canyon, has been excavated in the last few years. The archaeozoological and botanical analyses
437 carried out at Bavra-Ablari demonstrate that the Neolithic (layers dated to 6000-5350 BCE.) and
438 Chalcolithic populations (layers dated to 5000–3900 BCE.) occupying the rockshelter were clearly
439 engaged in a pastoral economy (Varoutsikos et al., 2017). Yet, the pollen spectra from the B9 unit at
440 Paravani does not reveal any signs that grazing impacted on the vegetation at that time (from 8000
441 to 5500 cal. BP). Moreover, significant impact of livestock on the vegetation has not been detected in
442 other regional pollen records. The main human impact recorded for this period is the extensive use
443 of fire during the Late Chalcolithic (Connor and Sagona, 2007; Connor 2011; Joannin et al. 2014). For
444 the Bronze Age period, several major sites have been excavated in the Samskhe-Javakheti region. The
445 plateau has yielded numerous sites from the Kura-Araxes culture (Early Bronze Age) and from the
446 Middle Bronze Age. The results of investigations carried out on Early Bronze Age sites (Kura-Araxes)
447 point to the development of “high mountain agriculture” marked by the importance of cereal
448 growing (Kvavadze and Kakhiani, 2010; Kakhiani et al., 2015, Messenger et al., 2015). The agro-
449 pastoral activities of these populations might have affected the Samskhe-Javakheti environment.
450 However, the Paravani pollen does not record any significant sign of cereal growing or of forest
451 clearance at that time. There may be various reasons for this discrepancy. Pollen records from large
452 lakes such as Paravani mostly reflect changes on a regional scale. This is why pollen assemblages are
453 significantly marked by forests while the signal of human impact is slight. Even if Kura-Araxes sites,
454 dedicated to an agricultural economy, are “frequent” on the Plateau, their environmental impacts
455 were probably not very large in scale and the signal of the environmental perturbations would have
456 been diluted in the regional pollen rain. The location of the sites in the watershed (or not), may also
457 have a major influence on our capacity to detect the intensity of human activities. If we consider the
458 pollen spectra from the C12 unit, the values for pollen indicators of human impact are a little bit
459 higher than in the contemporaneous base of unit B9, and are manifested as a slight increase of
460 *Plantago* and *Cerealia*. The origin of this unit of rapid sedimentation (Fig. 5) is not well understood,
461 but it seems that the deposition process allowed a better record of human impact than the sediment
462 deposited in the middle of the lake (unit B9 from PAR09-01). At the end of unit B9 (and
463 contemporaneous with unit D12), pollen spectra record an increasing human impact and the first
464 noticeable decline in trees (around 2000 cal. years BP).

465

466

From 1600 cal. years BP to the present

467 This last phase is recorded both in PAR12-04 (unit E12) and PAR09-01 (unit C9). It was deposited
468 between 1600-1500 cal. years BP and the present time (Fig. 7). These units are composed of an
469 organic rich sediment, indicating that the lake was still productive (Fig. 8). Diatoms remain well-
470 represented. While organic matter is abundant, the magnetic susceptibility is high in both of these
471 units. For this phase, PAR09-01 and PAR12-04 display different XRF curves for Al, Si, Ti and Fe. These
472 elements decrease throughout unit C9, although the same elements increase in unit E12, up to 10
473 cm. Thereafter these elements display a decreasing trend for the last 50-100 years (Fig. 3). Therefore,
474 for this phase, it is still difficult to reconstruct the erosion processes based on the XRF core scanner
475 data. According to pollen indicators of human impact (Fig. 8), the last 1500 years are marked by an
476 increasing anthropic imprint. For example, the taxon *Plantago*, a good marker of grazing, presents its
477 highest values in this phase (Fig. 6). Cereal pollen is also well represented. Wheat and barley are
478 mainly self-pollinating plants and their large pollen grains are not well-dispersed by the wind; hence,
479 cereal pollen abundances greatly decrease with distance from cultivated areas. Thus, the *Cereal*
480 values in the last Paravani phase probably indicate cereal growing within the Paravani watershed (up
481 to 2000m asl). Nowadays, cereals are still grown at this altitude on the Javakheti Plateau; some local
482 varieties of wheat, for example, are cultivated between 800 and 2160m asl (Akhalkatsi, 2016). The
483 decline in tree values initiated during the previous phase continues into the beginning of this phase.
484 The very top of the sequence observed in unit C9 is marked by a scarcity of deciduous trees. It is still
485 difficult to discuss the evolution of the tree cover on the plateau due to the additional pollen rain
486 coming from lower vegetation belts (Kvavadze, 1993; Connor et al., 2004). According to the botanists
487 that have worked on the region (Nakhutsrishvili, 1999; Arabuli et al, 2008), the expansion of the
488 mountain steppes on the Javakheti Plateau is a recent phenomenon, induced by late Holocene
489 deforestation. Certain archival sources, dating back to the 18th century, attest to a forested landscape
490 and thus support this hypothesis (Matcharashvili et al., 2004; Connor, 2011). Based on the pollen
491 analysis, we can presume that the decline of trees on the plateau is a process initiated at least 2300-
492 2000 years ago, but the scarcity of trees is probably a more recent process. However, it remains
493 difficult to pinpoint when this change occurred due to the problem of mixed pollen rains. The
494 question of the origin of the deforestation is also unresolved. According to the pollen evidence, both
495 cereal growing and pastoralism have played a role in shaping the vegetation on the plateau. While
496 grazing is a major driver of the modern vegetation, the intensity of this activity in the past has never
497 been evaluated. Fire setting and mowing may also have played a role in the process of opening up
498 the landscape. In the Aligol and Imera records (both located on the neighbouring Tsalka Plateau,
499 1500 m asl) an increase in fires is recorded at the beginning of the Classical Era (starting around 2400
500 cal. BP) and carries on in the subsequent periods (Connor, 2011). The role of fire in the
501 disappearance of fir on this lowest plateau has previously been considered (Connor, 2011).

502 Additional studies are required in order to chronicle the role of fire in the highlands and to make
503 comparisons with the lower Tsalka plateau. Above all, coprophilous fungi or mammal DNA analyses
504 could be undertaken in order to reconstruct the pastoral history of the Javakheti plateau, and to
505 better decipher its role in the expansion of mountain steppe.

506

507 **Conclusion**

508 The sediment analysis undertaken on different cores from Lake Paravani reveals the complex history
509 of sediment deposition in the bottom of this puzzling lake. While the sequences are affected by
510 hiatuses, and composed of truncated units, the combination of sediment, organic matter and pollen
511 analysis, with the help of ¹⁴C dates, allows us to reconstruct the evolution of the
512 palaeoenvironments in the Paravani watershed over the past 12 000 years. Although the XRF core
513 scanner turned out not to be the most suitable tool to conduct geochemical analysis on the Paravani
514 lake sediment, it has provided the first indications regarding the functioning of the Lake system
515 during the time period in question. The erosion pattern and the lake functioning reconstructed for
516 the Early and Mid-Holocene are in agreement with the vegetation dynamic; both reflect the
517 evolution of the climatic parameters (passage from glacial conditions to post-glacial conditions). The
518 phase of transition between the glacial steppe and the temperate forest is characterised by the
519 expansion of grassland (Poaceae steppe) which replaced the preceding Amaranthaceae-
520 Chenopodiaceae steppe. This phase, not observed in the previous Paravani analysis, was recently
521 identified in the south Caucasus and can be related to a more widely recognized phase of the Early
522 Holocene in the Near East. For the late Holocene (up to 2300 cal. years BP), the pollen record
523 indicates a gradual increase in human impact, but considering the regional (large scale) picture
524 provided by the pollen data, it is still difficult to identify the intensity of the anthropization on the
525 highlands. This period is marked by a change in the sediment delivered to the lake, but the effect of
526 human activities on this erosive pattern is not sufficiently understood. It would be interesting to
527 further investigate the role of the highland populations during the last two millennia in terms of land
528 use and agricultural practices. This would undoubtedly enhance the discussion regarding the
529 processes leading to the deforestation of the Plateau and the subsequent expansion of the mountain
530 steppes which nowadays cover the highlands.

531

532

533 **Acknowledgements**

534

535 This research was partly supported by the "GATES, Georgian Ancient Transcaucasia: Environments
536 and Societies" LIA project, founded by the French Environment and Ecology Institute (InEE, CNRS),

537 and the ANR-12 JSH3-003-01 Orimil project, directed by E. Herrscher. Thanks to L. Perrin for his
538 significant contribution to the fieldwork logistics. Radiocarbon dates were partly provided by LMC14,
539 Gif-sur-Yvette. We express our gratitude to Rhoda Allanic for correcting the language. We are finally
540 grateful to reviewers for their suggestions that greatly contributed to improve this paper.

541

542 **References**

543

544 Akhalkatsi, M., 2016 Ancient Crops Continuing for an Extended Period in Samtskhe-Javakheti Region
545 of Georgia – a Review. *Agricultural Research & Technology: Open Access Journal*, Volume 3 (1).

546

547 Ammann, B., 2009. Reconstruction of vegetation as a tool to understand resources of the past. In:
548 Masserey, C. (Ed.) *News of ancient Colchis Archaeological paleobotanical and historical research*
549 *program in the Framework of Georgian and Swiss cooperation*. Adamantis Press, Caucasian Press,
550 Tbilisi. pp. 5-9.

551

552 Anderson, N., 1986. Diatom biostratigraphy and comparative core correlation within a small lake
553 basin *Hydrobiologia* 143: 105 -112

554

555 Arabuli, G., Kvavadze, El., Kikodze, D., Connor, S., Kvavadze, Er., Bagaturia, N., Murvanisze, M.,
556 Arabuli, T., 2008. The Krummholz beech woods of Mt. Tavkvetili (Javakheti Plateau, Southern
557 Georgia), a relict ecosystem. *Proceedings of the Institute of Zoology* 23, 194-213.

558

559 Atanassova, J., 2005. Palaeoecological setting of the western Black Sea area during the last 15 000
560 years. *The Holocene* 15 (4), 576-584.

561

562 Beaudoin, A.B., Reasoner, M.A., 1992. Evaluation of differential pollen deposition and pollen
563 focussing from three Holocene intervals in sediments from Lake O'Hara, Yoho National Park, British
564 Columbia, Canada: intra-lake variability in pollen percentages, concentrations and influx. *Review of*
565 *Palaeobotany and Palynology* 75, (1-2), 103-131.

566

567 Beck, C., Reyss, J.-L., Leclerc, F., Moreno, E., Feuillet, N., Barrier, L., et al. (2012). Identification of
568 deep subaqueous co-seismic scarps through specific coeval sedimentation in Lesser Antilles:
569 implication for seismic hazard. *Natural Hazards and Earth System Sciences* 12(5), 1755–1767.

570

571 Beug, H.-J., 2004. *Leitfaden der Pollenbestimmung für Mitteleuropa und angrenzende Gebiete*, Pfeil,
572 Munich.

573

574 Birks, H.J.B., Birks, H.H., 1980. *Quaternary Palaeoecology*, Edward Arnold, London.

575

576 Blaauw, M., 2010. Methods and code for 'classical' age-modelling of radiocarbon sequences.
577 Quaternary Geochronology 5, 512–518. <https://doi.org/10.1016/j.quageo.2010.01.002>
578

579 Blaauw, M., Christen, J.A., 2011. Flexible paleoclimate age-depth models using an autoregressive
580 gamma process. Bayesian Analysis. 6:3. pp 457-474.
581

582 Bohn, U., Gollub, G., Hettwer, C., 2000. Karte der natürlichen Vegetation Europas, Bundesamt für
583 Naturschutz Federal Agency for Nature Conservation, Bohn-Bad Godesberg.
584

585 Bottema, S., 1986. A late Quaternary pollen diagram from Lake Urmia (northwestern Iran). Review of
586 Palaeobotany and Palynology 47, 241-261.
587

588 Çağatay, M.N., Öğretmen, N., Damcı, E., Stockhecke, M., Sancar, Ü., Eriş, K.K., Özeren, S., 2014. Lake
589 level and climate records of the last 90ka from the Northern Basin of Lake Van, eastern Turkey,
590 Quaternary Science Reviews 104, 97-116.

591 Chapron, E., Simonneau, A., Ledoux, G., Arnaud, F., Lajeunesse, P., Albéric, P., 2016. French Alpine
592 Foreland Holocene Paleoseismicity Revealed by Coeval Mass Wasting Deposits in Glacial Lakes.
593 Submarine Mass Movements and their Consequences, V, 341-349.
594

595 Cohen, A.S., 2003. Paleolimnology. The history and evolution of lake systems. Oxford University
596 Press, New York
597

598 Connor, S., Colombaroli, D., Confortini, F., Gobet, E., Ilyashuk, B.P., Ilyashuk, E.A., van Leeuwen,
599 J.F.N., Lamentowicz, M., O van der Knaap, W., Malysheva, E., Marchetto, A., Margalitadze, N. Mazei,
600 Y., Mitchell, E.A.D., Payne, R.J., Ammann, B., 2018. Long term population dynamics - theory and
601 reality in a peatland ecosystem. Journal of Ecology, 1-51.
602

603 Connor, S. E., Sagona, A., 2007. Environment and society in the late prehistory of Southern Georgia,
604 Caucasus. In: Lyonnet, B., (Ed.) Les cultures du Caucase (VIe-IIIe millénaires avant notre ère) – Leurs
605 relations avec le Proche-Orient. Editions Recherche sur les Civilisations. Paris CNRS Editions. pp. 21-
606 36.
607

608 Connor, S.E., 2011. A Promethean Legacy: Late Quaternary Vegetation History of Southern Georgia,
609 the Caucasus. Peeters, Louvain
610

611 Connor, S.E., Kvavadze, E.V., 2008. Modelling late Quaternary changes in plant distribution,
612 vegetation and climate using pollen data from Georgia, Caucasus. *Journal of Biogeography* 36 (3),
613 529-545.
614

615 Connor, S.E., Ross, S.A., Sobotkova, A., Herries, A.I.R., Mooney, S.D., Longford, C., Iliev, I., 2013.
616 Environmental conditions in the SE Balkans since the Last Glacial Maximum and their influence on the
617 spread of agriculture into Europe. *Quaternary Science Reviews* 68, 200–215.
618

619 Connor, S.E., Thomas, I., Kvavadze, E., Arabuli, G.J., Avakov, G., Sagona, A., 2004. A survey modern
620 pollen and vegetation along an altitudinal transect in southern Georgia, Caucasus region. *Review of*
621 *Palaeobotany and Palynology* 129, 229-250.
622

623 de Klerk, P., Haberl, A., Kaffke, A., Krebs, M., Matchutadze, I., Minke, M., Schulz, J., Joosten, H., 2009.
624 Vegetation history and environmental development since ca 6000 cal yr BP in and around Ispani 2
625 (Kolkheti lowlands, Georgia). *Quaternary Science Reviews* 28, 890-910.
626

627 Dean, J.R., Jones, M.D., Leng, M.J., Noble, S.R., Metcalfe, S.E., Sloane, H.J., Sahy, D., Eastwood, W.J.,
628 Roberts, C.N. 2015. Eastern Mediterranean hydroclimate over the late glacial and Holocene,
629 reconstructed from the sediments of Nar lake, central Turkey, using stable isotopes and carbonate
630 mineralogy, *Quaternary Science Reviews*, 124, 162-174
631

632 Djamali, M., Akhiani, H., Andrieu-Ponel, V., Braconnot, P., Brewer, S., de Beaulieu, J.-L., Fleitmann, D.,
633 Fleury, J., Gasse, F., Guibal, F., Jackson, S.T., Lézine, A.-M., Médail, F., Ponel, P., Roberts, N., Stevens,
634 L.R., 2010. Indian summer monsoon variations could have affected the early-Holocene woodland
635 expansion in the Near East. *The Holocene* 20, 813-820.
636

637 Djamali, M., de Beaulieu, J.-L., Shah-hosseini, M., Andrieu-Ponel, V., Ponel, P., Amini, A., Akhiani, H.,
638 Leroy, S.A.G., Stevens, L., Lahijani, H., Brewer, S., 2008. A late Pleistocene long pollen record from
639 Lake Urmia, NW Iran. *Quaternary Research* 69 (3), 413-420
640

641 Fægri, K., Iversen, J., 1989. *Textbook of pollen analysis* (revised by Fægri, K., Kaland, P.E. and
642 Krzywinski, K.). John Wiley and Sons.
643

644 Fox, J., 2016. *Using the R Commander: A Point-and-Click Interface for R*, 1st ed. Chapman and
645 Hall/CRC. <https://doi.org/10.1201/9781315380537>

646

647 Girard, M., Renault-Miskovsky, J., 1969. Nouvelles techniques de préparations en palynologie,
648 appliquées à trois sédiments du Quaternaire final de l'Abri Cornille (Istres, Bouches-du-Rhone).
649 Bulletin de l'AFEQ 21 (4), 275-284.

650

651 Goeury, C., Beaulieu, J.L. de, 1979. A propos de la concentration du pollen à l'aide de la liqueur de
652 Thoulet dans les sédiments minéraux. Pollen Spores 21, 239-251.

653

654 Grimm, E., 1987. CONISS: a Fortran 77 Program for stratigraphically constraint cluster analysis by the
655 method of incremental squares. Computers and Geosciences 13, 13-35.

656

657 Hamon, C., Jalabadze, M., Agapishvili, T., Baudouin, E., Koridze, I., Messenger, E., 2016. Gadachrili
658 Gora: Architecture and organisation of a Neolithic settlement in the middle Kura Valley (6th
659 millennium BC, Georgia). Quaternary International 395, 154-169

660

661 Heiri, O., Lotter, A.F., Lemcke, G. 2001. Loss on ignition as a method for estimating organic and
662 carbonate content in sediments: reproducibility and comparability of results. Journal of
663 Paleolimnology 25, 101-110.

664

665 Huntley, B., Birks, H.J.B., 1983. An Atlas of Past and Present Pollen Maps for Europe: 0-13000 years
666 ago. Cambridge University Press, Cambridge.

667

668 Huttunen, P., Stober, J. 1980. Dating of palaeomagnetic records from Finnish lake sediment cores
669 using pollen analysis. Boreas, 9 (3), 193-202

670

671 Joannin, S., Ali, A. A., Ollivier, V., Roiron, P., Peyron, O., Chevaux, S., Nahapetyan, S., Tozalakyan, P.,
672 Karakhanyan, A., Chataigner, C., 2014. Vegetation, fire and climate history of the Lesser Caucasus: a
673 new Holocene record from Zarishat fen (Armenia), Journal of Quaternary Science 29, 70-82.

674

675 Jones, M.D., Roberts, C.N., Leng, M.J., 2007. Quantifying climatic change through the last glacial–
676 interglacial transition based on lake isotope palaeohydrology from central Turkey. Quaternary
677 Research 67, 463-473.

678

679 Kachakhidze, M., Kachakhidze, N., Kiladze, R., Kukhianidze, V., Ramishvili, G. 2003. Relatively small
680 earth-quakes of Javakheti Highland as the precursors of large earthquakes occurring in the Caucasus.

681 Natural Hazards and Earth System Science, Copernicus Publications on behalf of the European
682 GeosciencesUnion, 2003, 3 (3/4), pp.165-170. hal-00299012
683

684 Kadowaki S., Maher, L. Portillo, M., Albert, R.M. Akashi, C., Guliyev, F., Nishiaki, Y., 2015.
685 Geoarchaeological and palaeobotanical evidence for prehistoric cereal storage in the southern
686 Caucasus: the Neolithic settlement of Göytepe (mid 8th millennium BP), Journal of Archaeological
687 Science 53, 408-425.
688

689 Kakhiani, K., Sagona, A., Sagona, C., Kvavadze, E., Bedianashvili, G., Messenger, E., Martin, L.,
690 Herrscher, E., Martkoplshvili, I., Birkett-Rees, J., Longford, C., 2013. Archaeological Investigations at
691 Chobareti in southern Georgia, the Caucasus. Ancient Near Eastern Studies 50, 1-138.
692

693 Koning, E., Epping, E., and Van Raaphorst, W., 2002. Determining Biogenic Silica in Marine Samples by
694 Tracking Silicate and Aluminium Concentrations in Alkaline Leaching Solutions. Aquatic Geochemistry
695 8, 37–67.
696

697 Kuzucuoğlu, C., Christol, L., Mouralis, D., Doğu, A.F., Akköprü, E., Fort, M., Brunstein, D., Zorer, H.,
698 Fontugne, M., Karabiyikoğlu, M., 2010. Formation of the Upper Pleistocene terraces of Lake Van
699 (Turkey). Journal of Quaternary Sciences 25, 1124-1137.
700

701 Kvavadze E.V., 1993. On the interpretation of subfossil spore-pollen spectra in the mountains. Acta
702 Palaeobotanica 33, 347-360.
703

704 Kvavadze E.V., Connor, S.E., 2005. *Zelkova carpinifolia* (Pallas) K. Koch in Holocene sediments of
705 Georgia - an indicator of climatic optima, Review of Palaeobotany and Palynology 133, 69-89.
706

707 Kvavadze, E.V., Kakhiani, K., 2010. Palynology of the Paravani burial mound (Early Bronze Age,
708 Georgia). Vegetation History and Archaeobotany 19 (5-6), 469-478.
709

710 Lê, S., Josse, J., Husson, F., 2008. FactoMineR: An R Package for Multivariate Analysis. J. Stat. Soft. 25.
711 <https://doi.org/10.18637/jss.v025.i01>
712

713 Lebedev, V.A., Bubnov, S.N., Dudaury, O.Z., Vashakidze, G.T., 2008. Geochronology of Pliocene
714 Volcanism in the Dzhavakheti Highland (the Lesser Caucasus). Part 2: Eastern Part of the Dzhavakheti
715 Highland. Regional Geological Correlation Stratigraphy and Geological Correlation 16, 553-574.

716

717 Lemcke, G., Sturm, M., 1997. $\delta^{18}O$ and Trace Element Measurements as Proxy for the Reconstruction
718 of Climate Changes at Lake Van (Turkey): Preliminary Results. In: Dalfes, H.N., Kukla, G., Weiss, H.
719 (Eds.), *Third Millennium BC Climate Change and old World Collapse*, NATO ASI Series. Springer, Berlin
720 Heidelberg, pp. 653-678.

721

722 Leroy, S.A.G., Arpe, K., 2007. Glacial refugia for summer-green trees in Europe and S-W Asia as
723 proposed by ECHAM3 time-slice atmospheric model simulations. *Journal of Biogeography* 34, 2115-
724 2128.

725

726 Leroy, S.A.G., Lopez-Merino, L., Tudryn, A., Chalieu, F., Gasse, F., 2014. Late Pleistocene and Holocene
727 palaeoenvironments in and around the middle Caspian basin as reconstructed from a deep-sea core.
728 *Quaternary Science Reviews* 101, 91–110.

729

730 Leroy, S.A.G., Tudryn, A., Chalieu, F., Lopez-Merino, L., Gasse, F., 2013. From the Allerød to the mid-
731 Holocene: palynological evidence from the south basin of the Caspian Sea. *Quaternary Science*
732 *Reviews* 78, 77–97.

733

734 Leroyer, C., Joannin, S., Aoustin, D., Ali, A.A., Peyron, O., Ollivier, V., Tozalakyan, P., Karakhanyan, A.,
735 Jude, F., 2016. Mid Holocene vegetation reconstruction from Vanevan peat (south-eastern shore of
736 Lake Sevan, Armenia), *Quaternary International* 395, 5-18.

737

738 Litt, T., Krastel, S., Sturm, M., Kipfer, R., Örcen, S., Heumann, G., Franz, S.O., Ülgen, U. B., Niessen, F.,
739 'PALEOVAN', International Continental Scientific Drilling Program (ICDP): site survey results and
740 perspectives. *Quaternary Science Reviews* 28 (15-16), 1555-1567.

741

742 Litt, T., Pickarski, N., Heumann, G., Stockhecke, M., Tzedakis, P.C., 2014. A 600,000 years long
743 continental pollen record from Lake Van, eastern Anatolia (Turkey). *Quaternary Science Reviews* 104,
744 30–41.

745

746 Lyonnet, B., Guliyev, F., Bouquet, L. Bruley-Chabot, G., Samzun, A., Pecqueur, L., Jovenet, E.,
747 Baudouin, E., Fontugne, M. Raymond, P., Degorre, E., Astruc, L., Guilbeau, D., Le Dosseur, G.,
748 Benecke, N., Hamon, C., Poulmarc'h, M., Courcier, A., 2016. Mentesh Tepe, an early settlement of
749 the Shomu-Shulaveri Culture in Azerbaijan, *Quaternary International* 395, 170-183.

750

751 Matcharashvili, I., Arabuli, G., Darchiashvili, G., Gorgadze, G., 2004. Javakheti Wetlands: Biodiversity
752 and Conservation [In Georgian and English]. NACRES, Tbilisi, Georgia.
753

754 Margalitadze, N.A., 1995. Istoriia golotsenovoi rastitel'nosti Gruzii. Metsniereba, Tbilisi (in Russian).
755 Matcharashvili, I., Arabuli, G., Darchiashvili, G., Gorgadze, G., 2004. Javakheti Wetlands: Biodiversity
756 and Conservation. NACRES, Tbilisi.
757

758 Messenger, E., Belmecheri, S., von Grafenstein, U., Nomade, S., Ollivier, V., Voinchet, P., Puaud, S.,
759 Courtin-Nomade, A., Guillou, H., Mgeladze, A., Dumoulin, J.P., Mazuy, A., Lordkipanidze, D., 2013.
760 Late Quaternary record of the vegetation and catchment-related changes from Lake Paravani
761 (Javakheti, South Caucasus). *Quaternary Science Reviews* 77, 125-140.
762

763 Messenger, E., Nomade, S., Wilhelm, B., Joannin, S., Scao, V., von Grafenstein, U., Martkoplshvili, I.,
764 Ollivier, V., Mgeladze, A., Dumoulin, J.P., Mazuy, A., Belmecheri, S., Lordkipanidze, D., 2017. New
765 pollen evidence for a delay in post-glacial forest expansion in the South Caucasus, the Nariani record.
766 *Quaternary Research* 87, 121-132.
767

768 Nakhutsrishvili, G.S., 1999. The vegetation of Georgia (Caucasus). *Braun-Blanquetia* 15, 1-68.
769

770 Nomade, S., Scao, V., Guillou, H., Messenger, E., Mgeladze, A., Voinchet, P., Renne, P.R., Courtin-
771 Nomade, A., Bardintzeff, J.M., Ferring, R., Lordkipanidze, D., 2016. New $^{40}\text{Ar}/^{39}\text{Ar}$, unspiked K/Ar
772 and geochemical constraints on the Pleistocene magmatism of the Samtskhe-Javakheti highlands
773 (Republic of Georgia), *Quaternary International* 395, 45-59.
774

775 North Greenland Ice Core Project Members, 2004. North Greenland Ice Core Project Members High-
776 resolution record of Northern Hemisphere climate extending into the Last Interglacial period. *Nature*
777 431, 147-151.
778

779 Nutz, A., Schuster, M., Ghienne, JF. et al., 2018. Wind-driven waterbodies: a new category of lake
780 within an alternative sedimentologically-based lake classification. *Journal of Paleolimnology* 59 (2),
781 189–199.
782

783 Pickarski, N., Kwiecien, O., Djamali, M., Litt, T., 2015. Vegetation and environmental changes during
784 the last interglacial in eastern Anatolia (Turkey): a new high-resolution pollen record from Lake Van:
785 palaeogeography, Palaeoclimatology, Palaeoecology 435, 145-158.

786

787 Philip, H., Avagyan, A.V., Karakhanian, A.S., Ritz, J.-F., Rebai, S. 2001. Slip rates and recurrence
788 intervals of strong earthquakes along the Pambak-Sevan-Sunik fault (Armenia). *Tectonophysics* 343,
789 205-232.

790

791 R Core Team, 2018. R: A language and environment for statistical computing. R Foundation for
792 Statistical Computing. Vienna, Austria.

793

794 Ragueneau, O., Savoye, N., Del Amo, Y., Cotten, J., Tardiveau, B., Leynaert, A., 2005. A New Method
795 for the Measurement of Biogenic Silica in Suspended Matter of Coastal Waters: Using Si:Al Ratios to
796 Correct for the Mineral Interference. *Continental Shelf Research* 25, 697-710.

797

798 Ritz, J.-F., Avagyan, A., Mkrtchyan, M., Nazari, H., Blard, P.-H., Karakhanian, A., Philip, H., Balescu, S.,
799 Mahan, S., Huot, S., Munch, P., Lamothe, M., 2016. Active tectonics within the NW and SE extensions
800 of the Pampak-Sevan-Syunik fault: Implications for the present geodynamics of Armenia, *Quaternary*
801 *International* 395, 61-78.

802

803 Reille, M., 1992. Pollen et Spores d'Europe et d'Afrique du Nord. Laboratoire de Botanique Historique
804 et Palynologie. U.R.A. C.N.R.S. 1152, Marseille.

805

806 Reimer, P.J., Bard, E., Bayliss, A., Beck, J. W., Blackwell, P. G., Bronk Ramsey, C., Buck, C. E., Cheng, H.,
807 Edwards, R. L., Friedrich, M., Grootes, P. M., Guilderson, T. P., Haflidason, H., Hajdas, I., Hatt, C.,
808 Heaton, T.J., Hogg, A.G., Hughen, K.A., Kaiser, K.F., Kromer, B., Manning, S.W., Niu, M., Reimer, R.W.,
809 Richards, D.A., Scott, E.M., Southon, J.R., Turney, C.S.M., van der Plicht, J., 2013. IntCal13 and
810 MARINE13 radiocarbon age calibration curves 0–50000 years cal BP, *Radiocarbon* 55, 1869-1887.

811

812 Roberts, N., 2002. Did prehistoric landscape management retard the post-glacial spread of woodland
813 in Southwest Asia? *Antiquity* 76, 1002-1010.

814

815 Roberts, N., Reed, J.M., Leng, M.J., Kuzucuoğlu, C., Fontugne, M., Bertaux, J., Woldring, H., Bottema,
816 S., Black, S., Hunt, E., Karabyikoğlu, M., 2001. The tempo of Holocene climatic change in the eastern
817 Mediterranean region: new high-resolution craterlake sediment data from central Turkey. *The*
818 *Holocene* 11, 721-736.

819

820 Rossignol-Strick, M., 1995. Sea-land correlation of pollen records in the eastern Mediterranean for
821 the glacial-interglacial transition: biostratigraphy versus radiometric time-scale. *Quaternary Science*
822 *Reviews* 14, 293-315.

823

824 Ryabogina, N., Borisov, A., Idrisov, I., Bakushev, M., 2019. Holocene environmental history and
825 populating of mountainous Dagestan (Eastern Caucasus, Russia). *Quaternary International* 516, 111-
826 126.

827

828 Sabatier, P., Dezileau, L., Briquieu, L., Colin, C., Siani, G., 2010. Clay minerals and geochemistry
829 record from northwest Mediterranean coastal lagoon sequence: implications for paleostorm
830 reconstruction. *Sediment. Geol.* 228, 205–217.

831

832 Shumilovskikh, L., Tarasov, P., Arz, H.W., Fleitmann, D., Marret, F., Nowaczyk, N., Plessen, B., Schlütz,
833 F., Behling, H., 2012. Vegetation and environmental dynamics in the southern Black Sea region since
834 18 kyr BP derived from the marine core 22-GC3. *Palaeogeography, Palaeoclimatology, Palaeoecology*
835 337-338, 177-193.

836

837 Stevens, L.R., Ito, E., Schwalb, A., Wright, H.E., 2006. Timing of atmospheric precipitation in the
838 Zagros Mountains inferred from a multi-proxy record from Lake Mirabad, Iran. *Quaternary Research*
839 66, 494-500.

840 Stevens, L.R., Wright, H.E., Ito, E., 2001. Proposed changes in seasonality of climate during the
841 Lateglacial and Holocene at Lake Zeribar, Iran. *The Holocene* 11, 747-755.

842

843 Turner, R., Roberts N., Eastwood W.J., Jenkins, E., Rosen, A., 2010. Fire, climate and the origins of
844 agriculture: micro-charcoal records of biomass burning during the last glacial-interglacial transition in
845 Southwest Asia. *Journal of Quaternary Science* 25, 371-386.

846

847 Van Zeist, W., Bottema, S., 1977. Palynological investigations in western Iran. *Palaeohistoria* 24, 19-
848 85.

849 van Zeist, W., Bottema, S., 1991. Late Quaternary vegetation of the Near East. *Beihefte zum Tubinger*
850 *Atlas des Vorderen Orients, Reihe A18, Wiesbaden: Dr L. Reichert Verlag, 156 pp.*

851

852 Varoutsikos, B. Mgeladze A., Chahoud, J., Gabunia, M., Agapishvili, T., Martin, L., Chataigner, C.,
853 2017. From the Mesolithic to the Chalcolithic in the South Caucasus: New data from the Bavra Ablari
854 rock shelter. In: Batmaz A., Bedianashvili G., Michalewicz A.,Robinson A. *Context and Connection:*

855 Essays on the Archaeology of the Ancient Near East in Honour of Antonio Sagona. Leuven: Peeters,
856 2017.
857

858 Wick, L., Lemcke, G. Sturm, M., 2003. Evidence of Lateglacial and Holocene climatic change and
859 human impact in eastern Anatolia: high resolution pollen, charcoal, isotopic and geochemical records
860 from the laminated sediments of Lake Van, Turkey. *The Holocene* 13, 665-675.
861

862 Wilhelm, B., Vogel, H., Crouzet C., Etienne, D. and Anselmetti, F.S. 2016a. Frequency and intensity of
863 palaeofloods at the interface of Atlantic and Mediterranean climate domains. *Climate of the Past*, 12,
864 299-316
865

866 Wilhelm, B., Nomade, J., Crouzet, C., Litty, C., Sabatier, P., Belle, S., Rolland, Y., Revel, M.,
867 Courboulex, F., Arnaud, F., Anselmetti, F.S. 2016b. Quantified sensitivity of lake sediments to record
868 historic earthquakes: Implications for paleoseismology. *Journal of Geophysical Research*, 121(1), 2–
869 16.
870

871 Wright, H.E., Jr, Ammann, B., Stefanova, I., Atanassova, J., Margalitadze, N., Wick, L., Blyakharchuk,
872 T., 2003. Lateglacial and Early-Holocene dry climates from the Balkan peninsula to southern Siberia.
873 *Aspects of palynology and palaeoecology* (ed. by S. Tonkov), Pensoft, Sofia-Moscow, pp. 127-136.
874

875 **Figure captions**

876

877 Figure 1: Geological map of the Javakheti Plateau, locations of cores PAR09-01 and PAR12-04 in Lake
878 Paravani (modified from Nomade et al., 2016).

879

880 Figure 2. Vegetation map of the region, (prepared using EuroVegMap software, Bohn et al., 2000).

881

882 Figure 3. Lithology, LOI analysis, magnetic susceptibility and XRF data for cores PAR09-01 and PAR12-
883 04. Radiocarbon ages and locations are indicated along the stratigraphy.

884

885 Figure 4. Principal component analysis (PCA) performed on major elements (Al, Si, K, Ti, Ca and Fe
886 intensities) measured by XRF core scanner. The samples have been coloured by unit.

887

888 Figure 5. Age-depth Model of PAR12-04 and PAR09-01

889

890 Figure 6. Synthetic pollen diagram (+ CONISS analysis) of the PAR12-04 core

891

892 Figure 7. Puzzle made of Paravani lake sediment units

893

894 Figure 8. Correlations of the PAR12-04 and PAR09-01 sequences.

895

896 **Table captions**

897

898 Table 1. List of AMS ¹⁴C dates from cores PAR09-01 and PAR12-04.

899

900 Table 2. Description of PAR 12-04 and PAR 09-01 units

901

902 **Supplementary data captions**

903

904 Supplementary Figure 1. Physiographic map of the region, showing Paravani (yellow star) and pollen
905 records discussed in the text (white stars). (The map is adapted from GeoAtlas).

906

907 Supplementary Figure 2. XRF core scanner curves of two elements (K and Ti) and the ratio Si/Al for six
908 sequences collected in the Lake Paravani

909

910 Supplementary Figure 3. Si/Al ratio along the PAR12-04 core, and photos of microscopic slides of bulk
911 sediment prepared for each unit (red circles correspond to diatoms)

912

913 Supplementary Figure 4. Si/Al, Ti/Al and Fe/Al ratios along the PAR12-04 and PAR09-01 cores

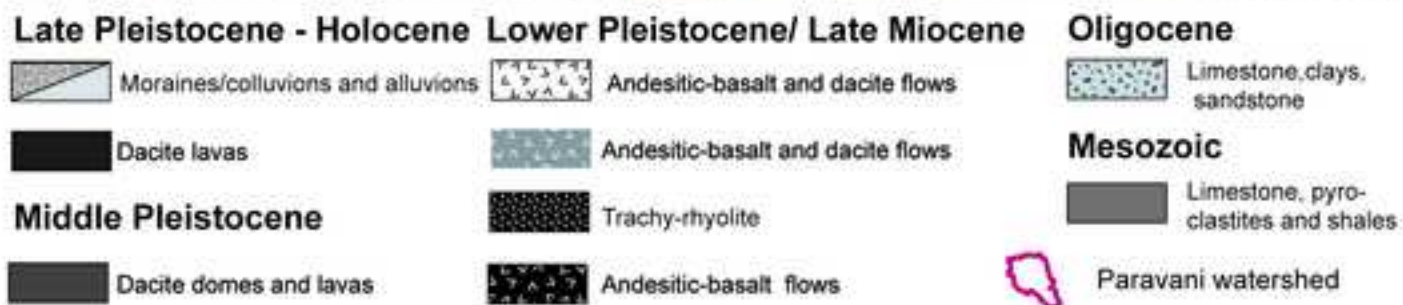
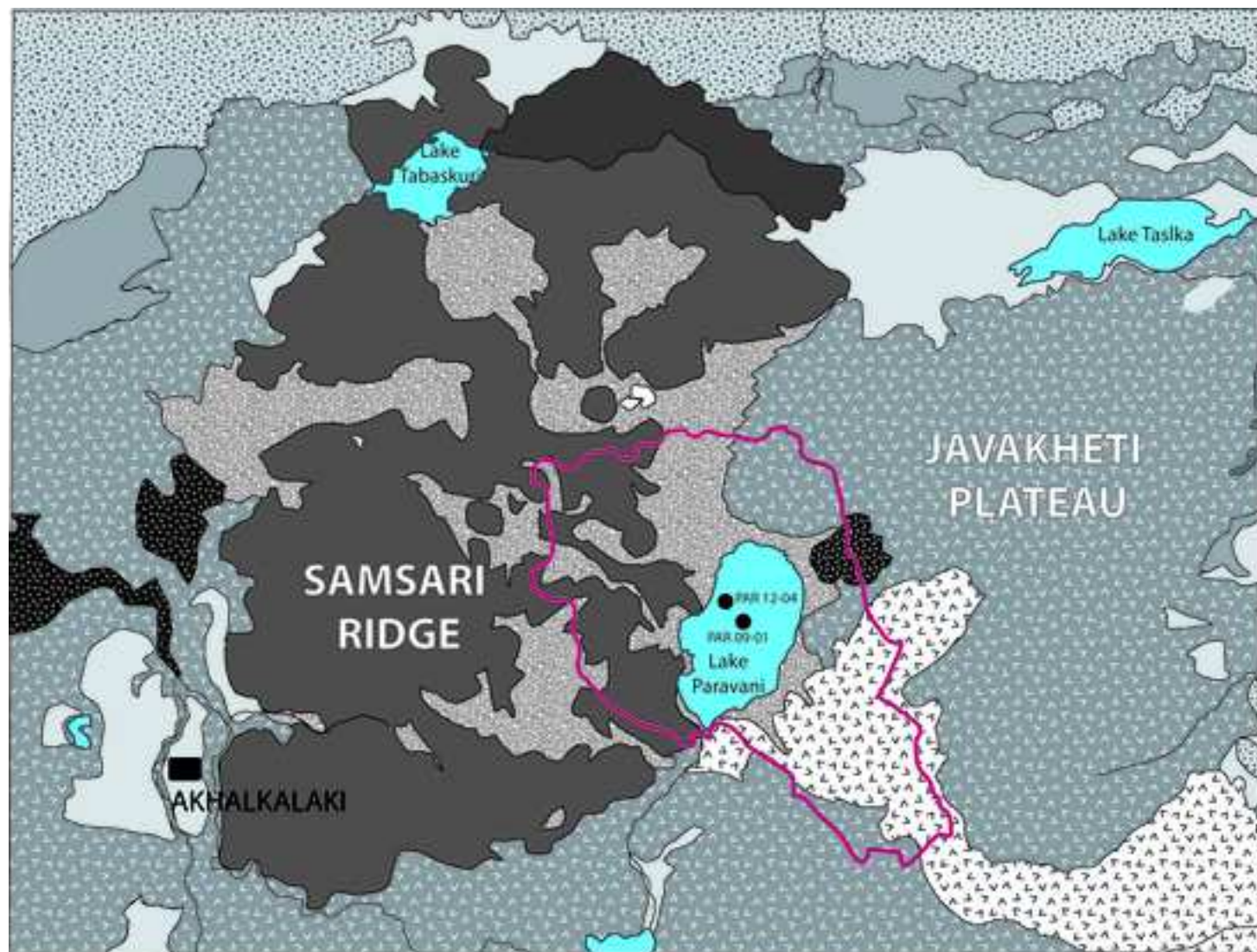
914

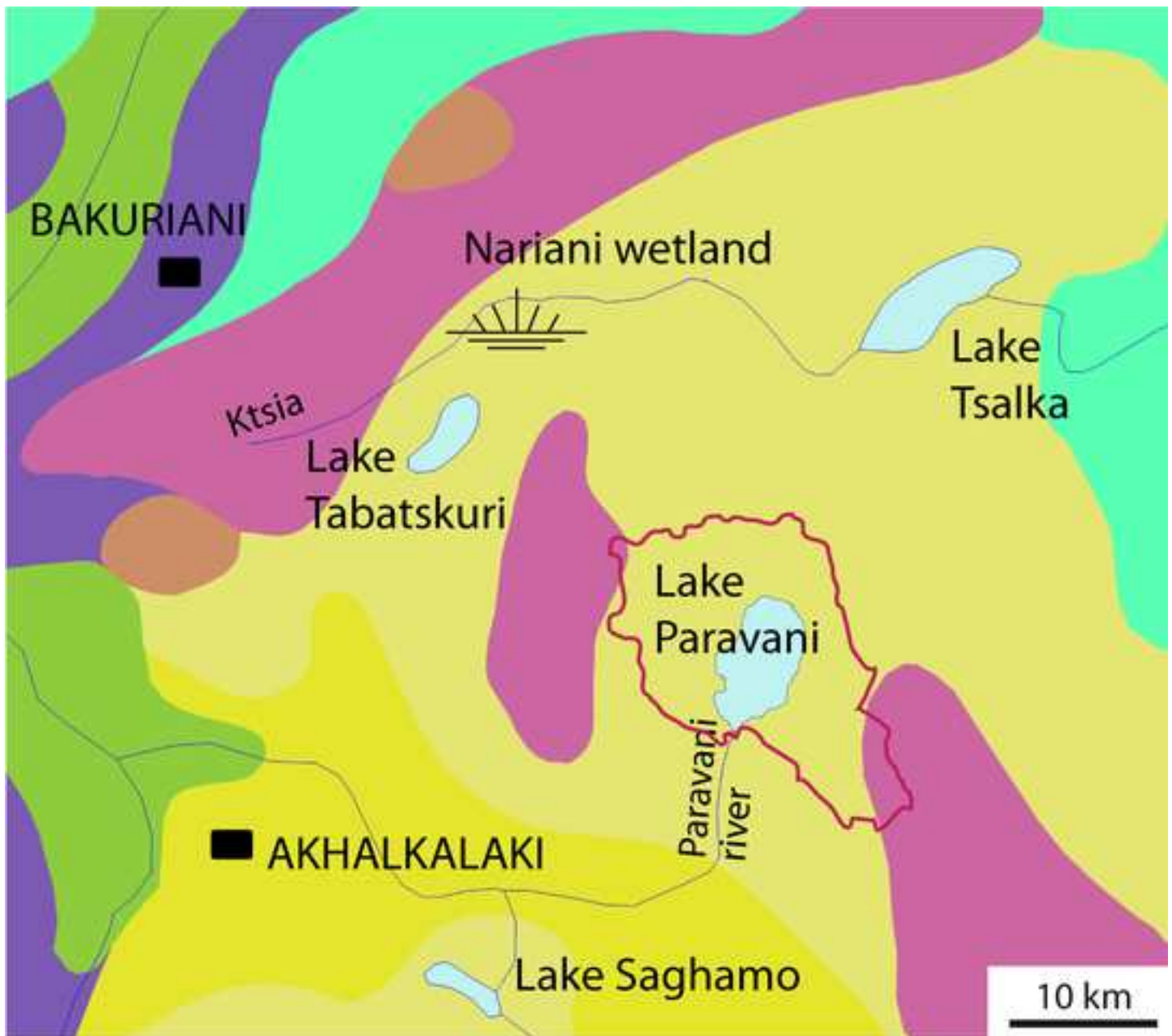
915 Supplementary Figure 5. Synthetic pollen diagram of PAR 12-04 and PAR 09-01 cores

916

917 Supplementary Figure 6. Comparison of regional pollen records (Arboreal Pollen, Poaceae and
918 steppic plants): Zarishat (Joannin et al., 2014), Van (Litt et al., 2012; Pickarski et al., 2015), Nariani
919 (Messenger et al., 2017), Paravani (this study) and Dedichara (Connor et al., 2018). The Paravani
920 synthetic curves are composed of PAR12-04 pollen data (lower part) and PAR09-01 pollen data
921 (upper part). The Dedichara pollen data are from the European Pollen Database, available in the
922 Neotoma Paleoecology Database.

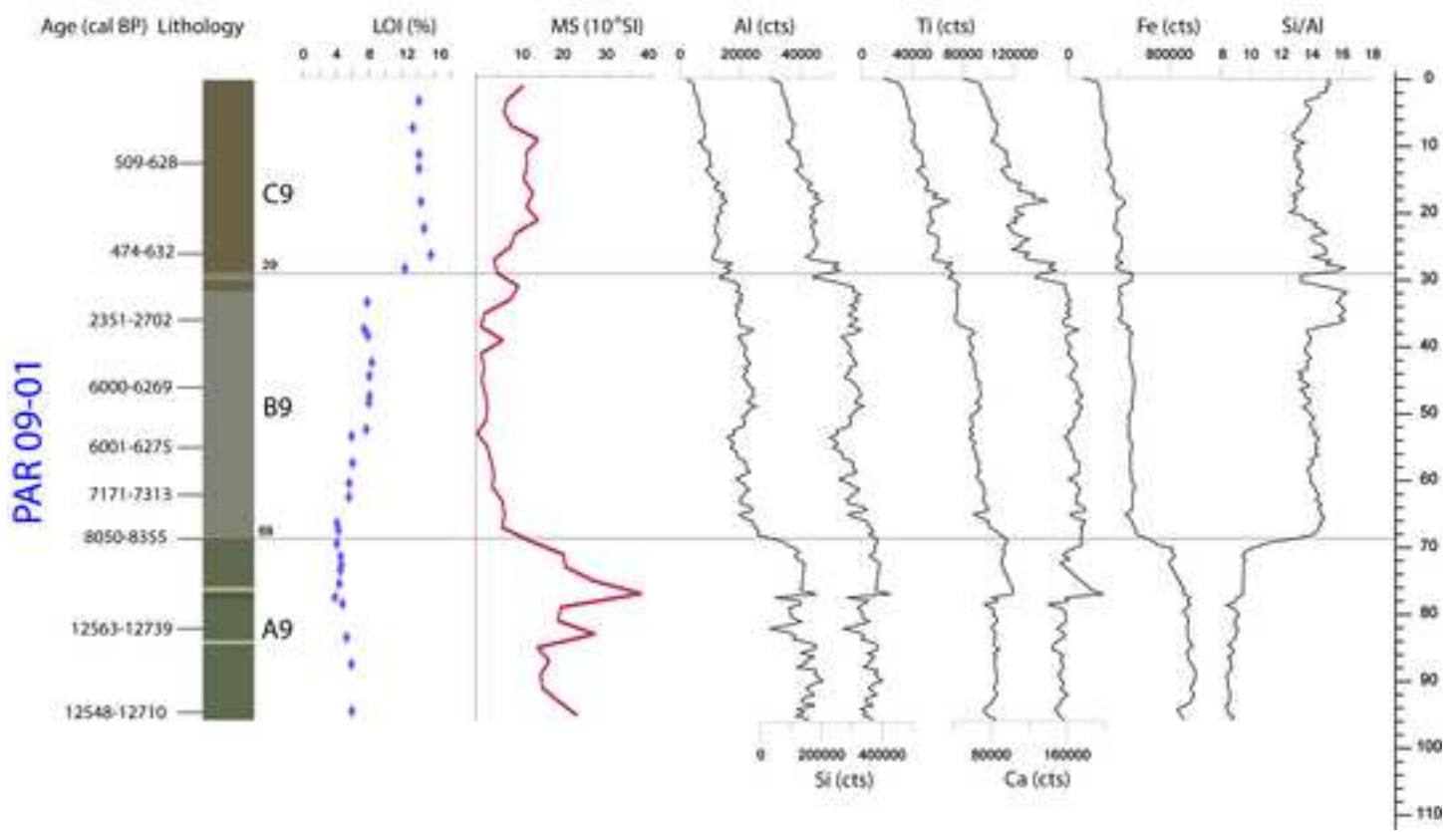
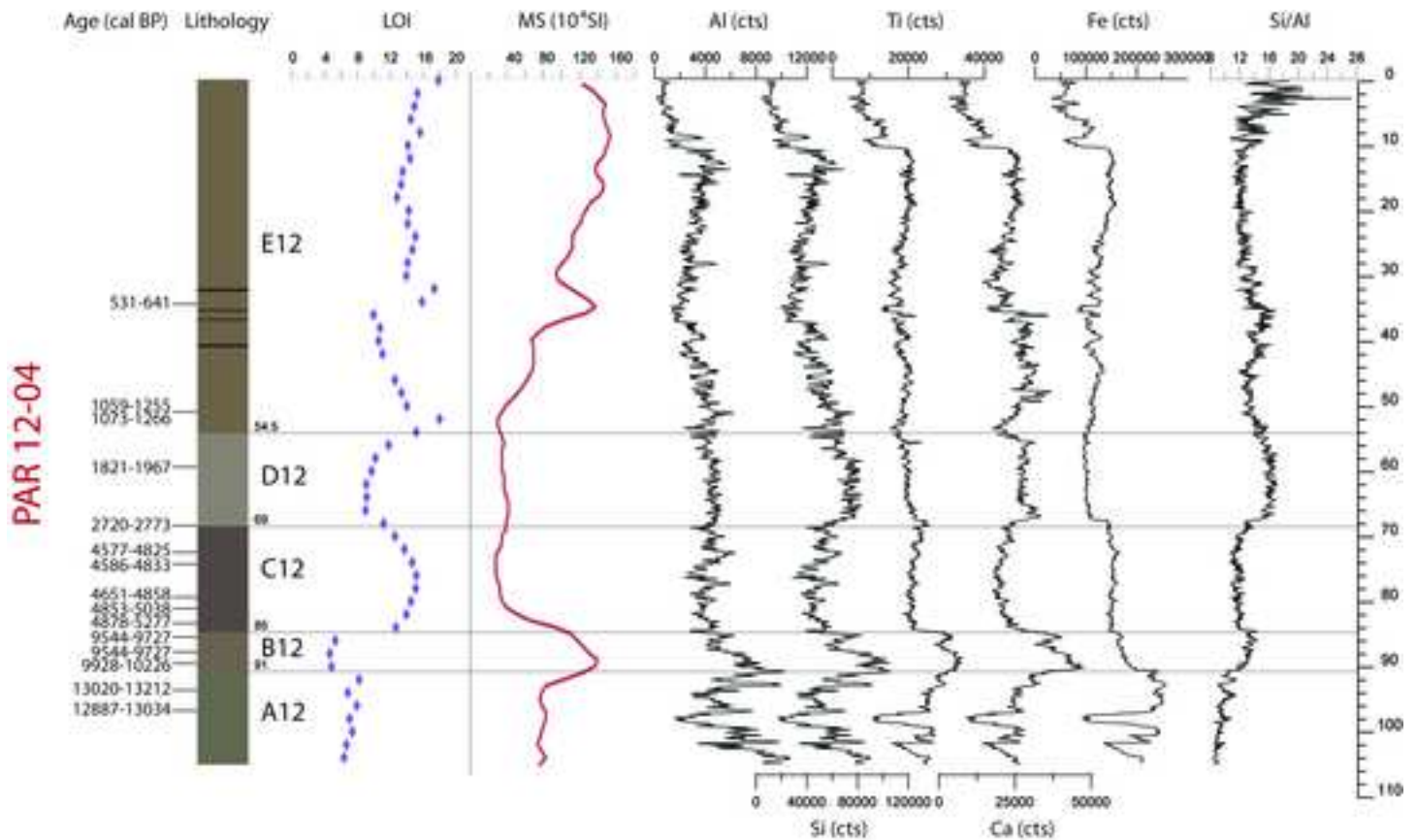
923

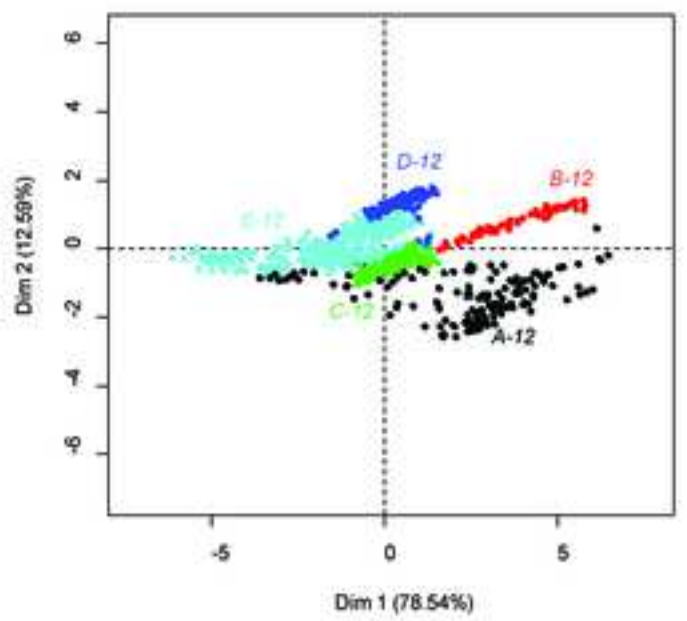
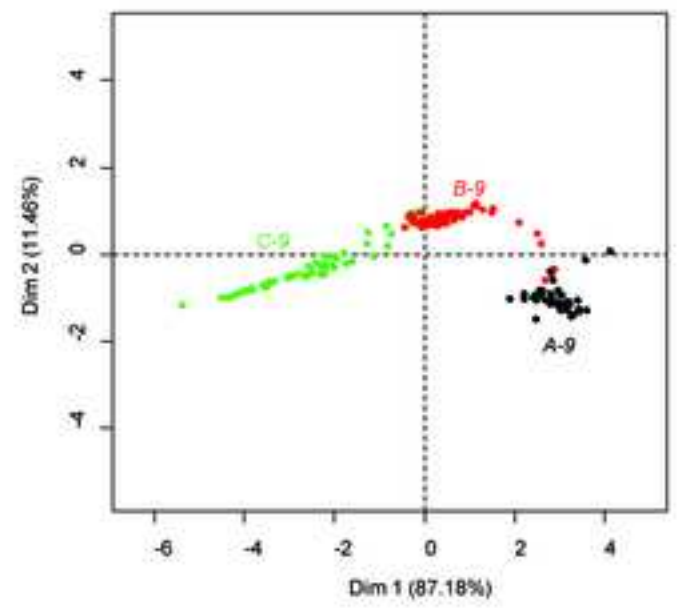
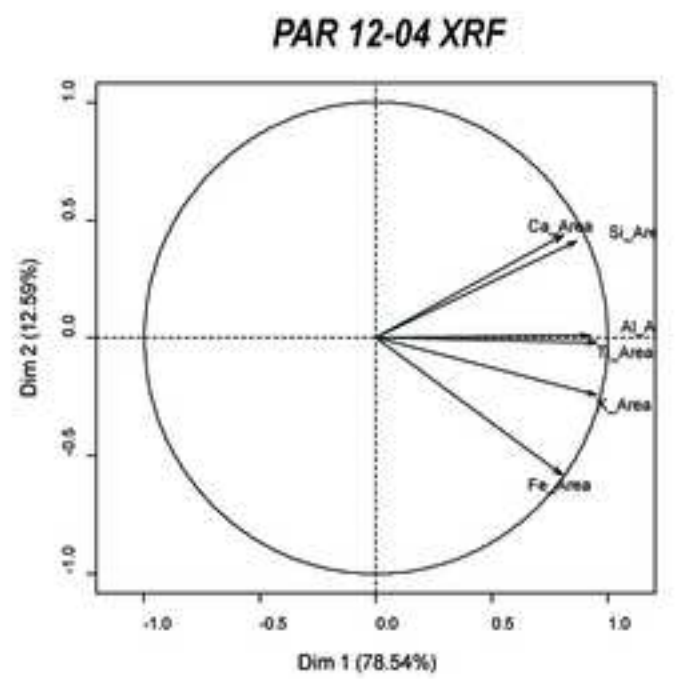
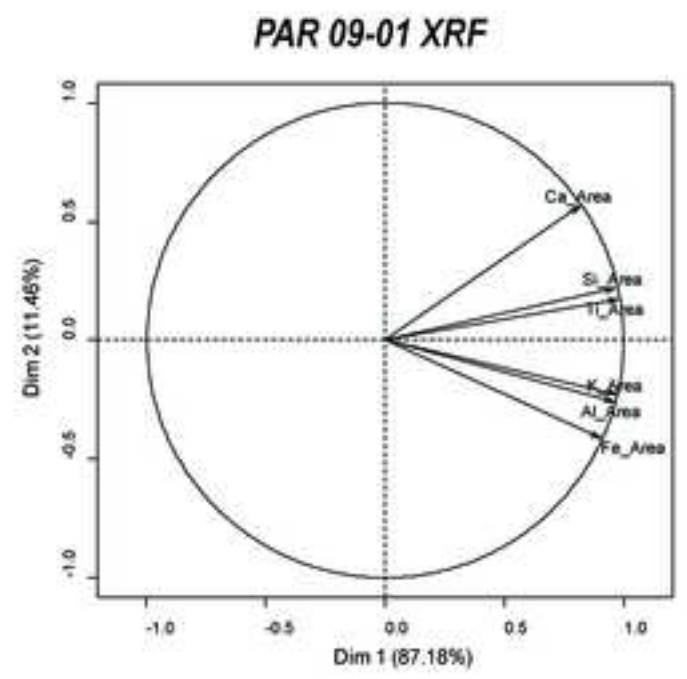


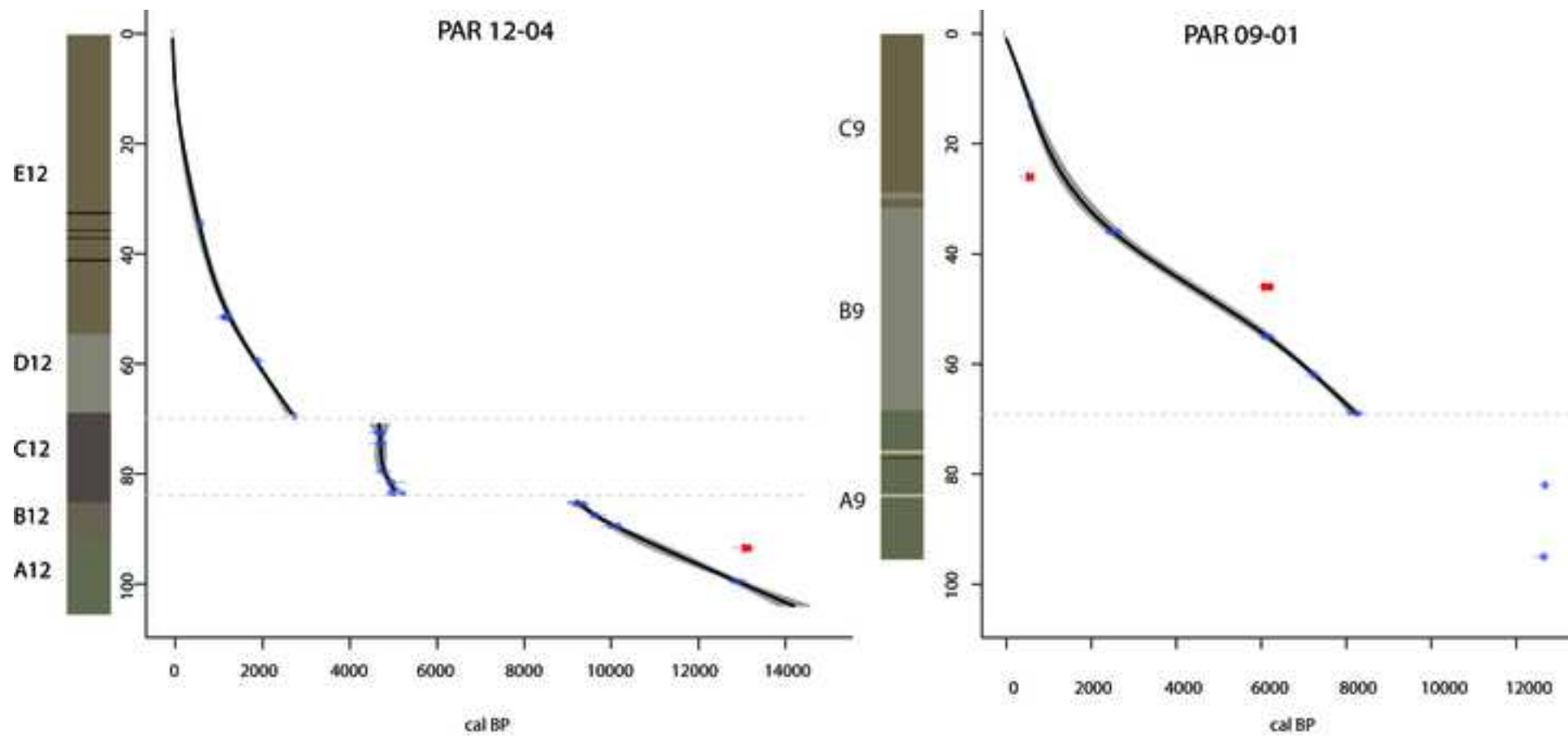


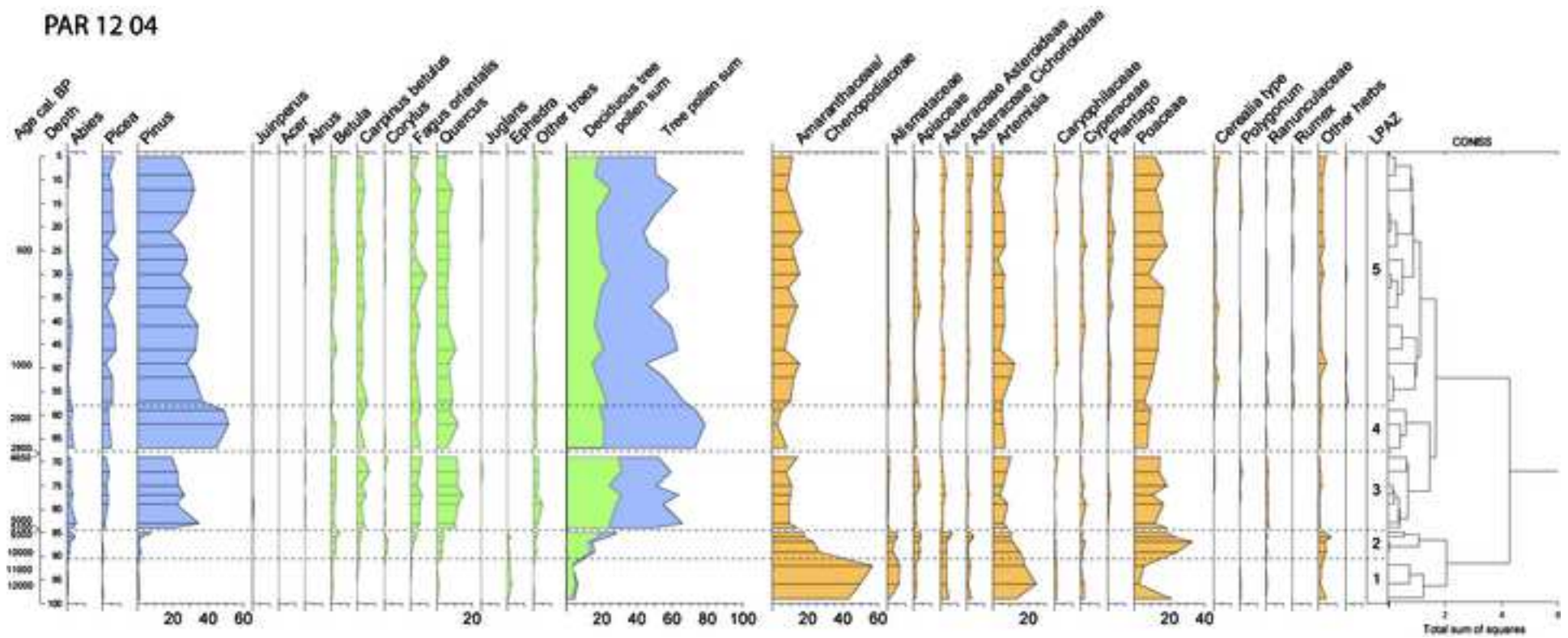
- | | | |
|--|--|---|
|  Krummholz and open woodland, scrub, tall forb communities, grasslands and true steppes |  Beech forests |  Main cities |
|  Pine forests |  Oak, hornbeam-oak and oriental hornbeam-oak forests | |
|  Altimontane herb-grass and meadow steppes |  Fir, spruce-fir, beech-fir forests, often alternating with beech forests | |
|  Montane Stipa steppes |  Paravani watershed | |

Figure 3









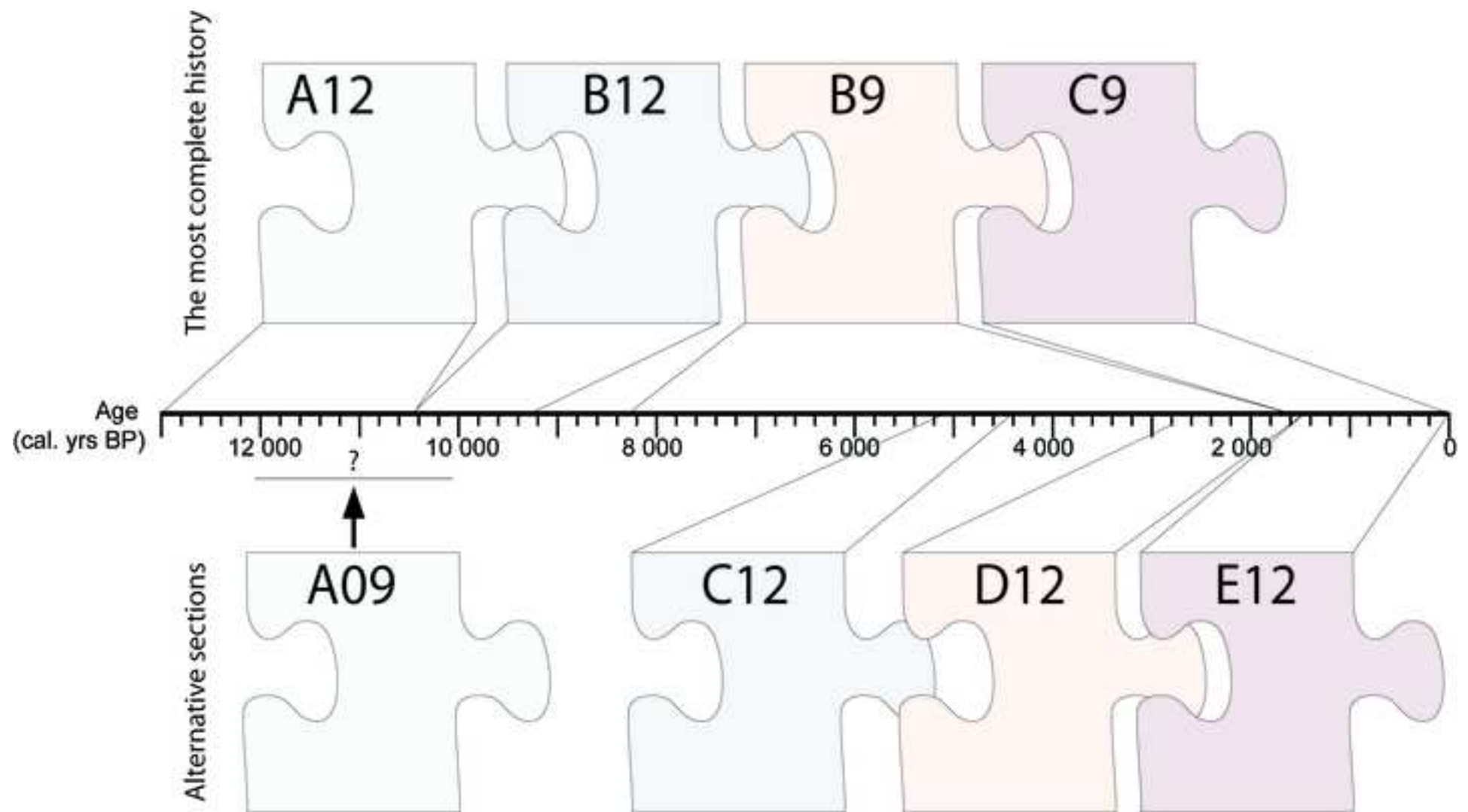
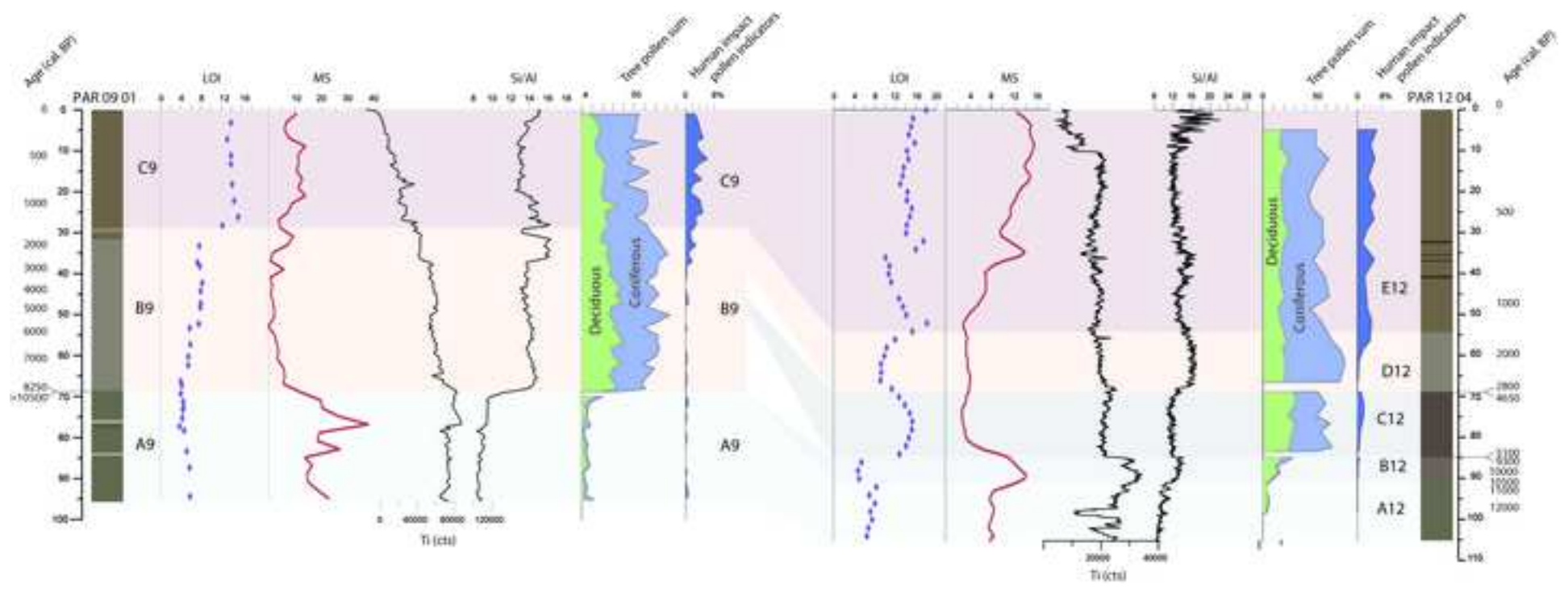


Figure 8





Click here to access/download

Table

Table 1.xlsx





Click here to access/download

Table

Table 2.xlsx





Click here to access/download
Data in Brief
Data in Brief Figs Sup.zip

